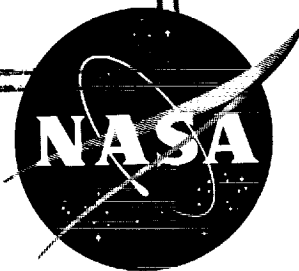


NASA TN D-1305

**CASE FILE
COPY**

N 62 13945
NASA TN D-1305



TECHNICAL NOTE

D-1305

EMISSION SPECTRA FROM HIGH-PRESSURE

HYDROGEN-OXYGEN COMBUSTION

By Marshall C. Burrows and Louis A. Povinelli

Lewis Research Center
Cleveland, Ohio

NATIONAL AERONAUTICS AND SPACE ADMINISTRATION
WASHINGTON

July 1962

NATIONAL AERONAUTICS AND SPACE ADMINISTRATION

TECHNICAL NOTE D-1305

EMISSION SPECTRA FROM HIGH-PRESSURE

HYDROGEN-OXYGEN COMBUSTION

By Marshall C. Burrows and Louis A. Povinelli

SUMMARY

Emission spectra were obtained from a nominal-200-pound-thrust gaseous-hydrogen - gaseous-oxygen combustor for the wavelength interval between 2100 and 7800 Angstroms (A); all mixtures were hydrogen-rich. The burning mixture was seen through quartz windows insulated by a film of dry nitrogen gas. Spectra were obtained by means of a grating spectrograph. It was equipped with a 20-inch photographic plate holder that allowed exposure of the entire wavelength interval at one time with a first-order dispersion of 10.9 A per millimeter.

Principal radiation between 2100 and 7800 A consisted of the hydroxyl bands extending from 2444 to 3546 A, the Schumann-Runge bands of oxygen between 2400 and 4600 A, and the sodium D lines at 5890 and 5896 A. There was evidence of background radiation throughout the wavelength interval.

The intensities of hydroxyl, oxygen, and continuum radiation increased in proportion to both the oxidant-fuel weight ratio and the pressure. Comparisons were made with results in the literature and a statistical theory. The rotational temperature of the hydroxyl radical was determined, and its accuracy is discussed. Sodium emission decreased in proportion to the length of the run; therefore, sodium must have been a contaminant in the hardware. The width of a hydroxyl line was measured; a mercury line was used for the comparison.

Comparative spectral data, taken of a tungsten-ribbon lamp operated at various temperatures, were used to obtain the spectral characteristics of the films and the relative intensities of the combustor spectra.

INTRODUCTION

Emission spectra from hydrogen-oxygen flames have been studied extensively in the laboratory at pressures from 0.01 to 1.0 atmosphere.

These data have been analyzed regarding the hydroxyl (OH) bands and their rotational temperatures (refs. 1 to 7), the Schumann-Runge bands of oxygen (O_2) and their excitation (ref. 8), the rotation-vibration bands of water (H_2O) (ref. 9), the rotation-vibration bands of OH in the infrared region (refs. 10 and 11), and the continuous spectrum (ref. 11). Early work had proved that the visible radiation from hydrogen-oxygen flames increased rapidly with pressure (ref. 12).

The literature does not contain any observations of hydrogen-oxygen flame spectra at the pressures and mass flows characteristic of rocket practice that show the comparative intensities of continuous spectra, spectra from atomic and molecular species, and spectra from contaminants present in the system. The present investigation was undertaken to obtain some quantitative information about the spectral intensity distribution of gaseous hydrogen and gaseous oxygen burning at high pressures and to gain additional insight into the physical and chemical processes occurring during rocket combustion.

Emission spectra were taken of the gases inside the combustor for various chamber pressures, total weight flows, oxidant-fuel weight ratios, and run lengths.

APPARATUS AND PROCEDURE

Combustor

The combustor (fig. 1) was designed for a nominal operating pressure of 450 pounds per square inch at a total weight flow of 0.6 pound per second and for gaseous hydrogen and oxygen propellants. The injector, the chamber, the windowed section, and the nozzle were separate units constructed of copper; they could be run uncooled for 2 to 4 seconds. A recessed sparkplug in the injector initiated combustion. Quartz windows recessed 1 inch from the chamber wall and constructed for purging with a film of dry gaseous nitrogen provided a view of the burning mixture. A critical-flow orifice was used in the nitrogen line so that the combustion gases were purged out of the cavity by a positive nitrogen flow of approximately 0.05 pound per second. The windows remained clear for viewing for approximately 50 seconds total running time. A white dusty film collected on the windows, but this could readily be removed.

Measured values of combustion pressure and total weight flow were used to determine the experimental characteristic velocity c^* for the runs. Measured c^* values for propellant flows from 0.2 to 0.6 pound per second were 98 ± 3 percent of the theoretical value corrected for the nitrogen flow.

Spectrographic Components

The spectrograph was a 1.5-meter Wadsworth grating instrument equipped with a 35-millimeter film holder and a remotely operated shutter (fig. 2). The 15,000-groove-per-inch grating could display a wavelength range of 2100 to 7800 Å in the first order, 2100 to 3900 Å in the second order, and 2100 to 2600 Å in the third order. Reciprocal linear dispersion at the film holder was 10.9 Å per millimeter in the first order, 5.45 Å per millimeter in the second order, and 3.63 Å per millimeter in the third order.

Lenses or mirrors were used to focus the radiation from the 1/2-inch combustor window on the entrance slit of the spectrograph; the image was reduced at the entrance slit to 2 millimeters in height. Glass optics limited the range of the instrument to approximately 3100 to 7800 Å in the first order and 3100 to 3900 Å in the second order. Quartz lenses or uncoated front surface mirrors transmitted the full wavelength range.

EXPERIMENTAL RESULTS AND DISCUSSION

The spectra of the hydrogen-oxygen combustion gases show lines caused by OH (2444 to 3546 Å) and part of the Schumann-Runge system of O₂ (2400 to 4400 Å) (fig. 3(a)). A continuum extends over the entire wavelength span of the spectrograph. The only contaminant in the system appears to be sodium, which has emission lines at 5890 and 5896 Å.

Since excess hydrogen was present in all runs, the spectra were examined for lines that were caused by atomic and molecular hydrogen. The emission spectrum of hydrogen (H) (Balmer series) mainly consists of lines at 4101.7, 4340.5, 4861.3, and 6562.8 Å. The spectrum formed by molecular hydrogen consists of the aforementioned lines together with many fine lines and a continuum extending from wavelengths shorter than 3000 Å to those of approximately 4500 Å. The spectra from the combustion gases reveal lines at 4102 and 4340 Å that could be due to H or H₂. The continuum that extends over the entire wavelength range is apparently due to H₂, O₂, or ionized sodium (Na) (fig. 3(b)). The elimination of higher order overlap by means of filters revealed that this continuum extends beyond 6100 Å (fig. 3(c)).

Attempts to photographically record infrared spectra (7000 to 7800 Å) of OH, O₂, and H₂O were not successful, this could be due because of either lower sensitivity of the infrared film or decreased radiation in this wavelength region.

Variation of Spectral Intensities with Combustion

Pressure and Total Weight Flow

The spectral intensities of the combustion gases changed considerably with the increase in pressure and in total weight flow (fig. 4). In order to obtain these data, the propellant flow was increased while the oxidant-fuel weight ratio and the nozzle diameter were held constant. These spectra were analyzed on a recording microphotometer, and the resulting transmission values were converted to intensities. The change in the intensity with pressure and weight flow is shown as a function of wavelength by the faired curves in figure 5. The most intense radiation was between 3100 and 3600 Å, with the continuum strongly depending on the pressure in the visible region. The curves were not extended to wavelengths longer than 6200 Å because of the reduced film sensitivity after that point.

Figure 6 shows the effect of pressure on radiation intensity at selected wavelengths. These wavelengths correspond to the OH line at 3258 Å (${}^2\Sigma - {}^2\Pi$, 2, 2) the O₂ line at 3571 Å and the continuum at 3574 Å. On account of the wide spacing between the O₂ lines, independent measurement of the continuum intensity was possible. Thus, the intensity of the continuum could be subtracted from the O₂ line intensity at each pressure. The curves indicate that the pressure exponent of the intensity of Schumann-Runge O₂ radiation varied from 2.6 at 150 pounds per square inch absolute to 2.0 at 325 pounds per square inch absolute. At 425 pounds per square inch absolute the intensity approached a constant. The intensity of the continuum increased more rapidly with pressure than did the Schumann-Runge emission of O₂. The pressure exponent of the continuum radiation intensity decreased from 3.2 at 150 pounds per square inch absolute to 2.4 at 450 pounds per square inch absolute.

Liveing and Dewar (ref. 12) studied flames in a chamber with H₂ and O₂ inlets perpendicular to one another. Observations were made through a quartz window at the end of the chamber. For flames of O₂ in H₂ the blue radiation increased in relation to the square of the pressure in the range 15 to 95 pounds per square inch absolute. The pressure exponent is compatible with the results of the present study.

Liveing and Dewar also discovered that the flames of H₂ in O₂ were bright but their luminosity increased less rapidly with pressure. Gaydon (ref. 11) based his explanation of this difference on the fact that O₂ in excess of H₂ mainly produces the continuum, which depends on the pressure squared. On the other hand, H₂ in O₂ produces a higher Schumann-Runge emission, which increases less rapidly with pressure.

Variation of Spectral Intensities with Oxidant-Fuel Weight Ratio

The appearance of the spectra changed very little in comparison with the changes in the oxidant-fuel weight ratio, o/f (fig. 7). When the spectra were analyzed on a microphotometer, the gross spectral intensities for the three oxidant-fuel weight ratios varied as indicated by the faired curves of figure 8. The spectral characteristics were similar for the three oxidant-fuel weight ratios; the most intense radiation occurred between 3100 and 3600 Å. A continuum over the entire wavelength range was accompanied by the sodium D lines.

The variation of the intensities with oxidant-fuel weight ratio is shown in figure 9 for two OH lines, an O₂ line, and the continuum. Once again, it was possible to separate the contribution of the O₂ line from that of the continuum. Radiation intensity consistently increased with the oxidant-fuel-weight ratio for values less than the stoichiometric ratio of 8.

The overall effect of the oxidant-fuel weight ratio on the radiation intensity was much less than that of pressure. An oxidant-fuel weight ratio variation from 3.5 to 7.0 increased the radiation intensity 2.6 times for the O₂ line at 3571 Å; however, when pressure was doubled the radiation intensity increased 5.4 times. Theoretical variations of intensity with oxidant-fuel weight ratio, as well as the experimental curves for OH and O₂ are shown in figure 10. The theoretical curves are based on the assumption that the Beer-Lambert Law holds for the emissivity ϵ_λ according to the equation:

$$\epsilon_\lambda = 1 - e^{-k_\lambda n L P} \quad (1)$$

where

k_λ absorption coefficient of radiation, (cm⁻¹)(atm⁻¹)

L beam length, cm

n mole fraction

P total pressure, atm

Mole fractions of the absorbing gases, OH and O₂, have been obtained from thermochemical calculations as functions of the oxidant-fuel weight ratio for equilibrium combustion conditions (Unpublished NASA data by Sanford Gordon) and are shown in table I together with other necessary data.

The curves in figure 10 show wide differences between the experimental and theoretical data. One explanation for those differences suggests that the radiation could have been excited nonthermally. It has been shown that the rotational temperature of the OH radical in the inner cone of a hydrocarbon flame is much higher than the theoretical flame temperature, which indicates some chemiluminescence (ref. 10). This behavior has also been observed in the hydrogen flame at atmospheric pressure (ref. 13). A second explanation for the difference in the curves shown in figure 10 suggests that the propellants were not uniformly mixed in the combustor. The injector produced a turbulent gas stream with a random formation of eddies, whose initial composition was a function of position and whose scale was distributed over a wide range. The flow stream, composed of these eddies or striations, probably burned at various oxidant-fuel weight ratios and, thus, produced a distribution in the temperature and the composition of the radiating gas stream.

The variation of the oxidant-fuel composition of the eddies was assumed to follow a log normal distribution, dn/dy , according to the relation

$$\frac{dn}{dy} = \left(\sqrt{2\pi} \sigma e^{y^2/2\sigma^2} \right)^{-1} \quad (2)$$

where

n frequency of occurrence

y $\ln \frac{o/f}{(o/f)_{\text{mean}}}$

σ distribution factor, ratio of o/f at probability of 0.84 to $(o/f)_{\text{mean}}$

When the metered oxidant-fuel weight ratio was taken as the $(o/f)_{\text{mean}}$ and the distribution factor σ was assumed equal to 1.6, the theoretical variation of intensity with o/f corresponded closely to the experimental values obtained for the OH and O_2 intensities (figs. 10 and 11).

The level of the theoretical curve was matched to the experimental data points using relative values of intensity from table 1.

Previous measurements of rocket combustor temperatures utilizing an optical technique show a smaller variation in time- and space-averaged temperatures than was predicted on the basis of the metered oxidant-fuel weight ratio (refs. 14 and 15). However when velocity-of-sound technique (ref. 16) was used to measure instantaneous flow properties in a small combustor, wide variations in the temperature-molecular-weight ratios were found. These time and space variations in the radiation,

the temperature, and the composition imply that rocket combustion is a phenomenon undergoing various degrees of reaction (viz., striations on pockets of gases) throughout the burning region. This physical interpretation of the combustion zone was advanced previously for premixed turbulent flames (ref. 17). Investigation of the physical structure of turbulent flames has indicated that the flame zone may be both wrinkled and distributed in the degree of reaction (ref. 18). For low-intensity flames the structure can be predicted on the basis of velocity-ratio gradients or chemical- to turbulence-time ratio (ref. 19).

Rotational Temperature Measurement

The rotational temperature of the OH radical was determined from the intensity distribution of selected OH lines. References 1 to 7 and reference 20 discuss the techniques involved. Briefly, the technique that was used involved the measurement of the transition intensity I from a level K of a line near the head of a branch where I is given by

$$I = CA_K e^{-E_K/kT} \quad (3)$$

where

- C constant for a particular electronic and vibrational transition
- A_K transition probability from ref. 21
- E_K rotational energy level of initial state from ref. 20
- k Boltzmann's constant
- T rotational temperature

A second line of equal intensity was chosen in the tail of the same branch such that, at the first approximation, the lines were equally self-absorbed for a uniform temperature source, and errors in the intensity determination were cancelled. The rotational temperature was determined from the relation

$$T = \frac{E'_K - E_K}{K \ln \frac{A'_K}{A_K}}$$

where

$$K = 1 \text{ and } K' > 1.$$

The rotational temperature of the S_{21} lines of the OH radical was $3250^{\circ} \pm 400^{\circ}$ K. A plot of the intensities of the S_{21} lines as a function of transitional level K (fig. 12) determined that temperature. A band representing a ± 5 percent variation in the intensities was used to account for the spread in the data. Curves drawn within these limits, representing maximum and minimum variations in K , gave temperatures of 3650° and 2850° K, respectively. The average of these two temperatures was in reasonable agreement with the theoretical value of 3560° K for a stoichiometric mixture (Unpublished NASA data by Sanford Gordon).

An alternative technique was used to confirm the rotational temperature. Equation (3) can be written as

$$\log I = \log C + \log A_K - E_K/kT \quad (5)$$

If $\log I - \log A_K$ is plotted against E_K , the resulting curve should have a slope of $-kT$. This method was used for several branches of the OH spectra from the engine data; however, the resulting curve was not linear, and the temperatures determined from the slope ranged from less than 1000° to more than $10,000^{\circ}$ K. The factors leading to these values may have been (1) self-absorption, (2) continuous background, (3) large errors in the quantitative intensity determination, or (4) non-rotational equilibrium.

Both methods of obtaining the rotational temperature were checked for the above factors by applying them to spectra obtained from the outer cone of an oxyacetylene flame. A comparison of the spectra (fig. 13) showed large differences in the region of 3064 Å.

The R_2 lines could easily be distinguished in the oxyacetylene flame, and the rotational temperature determined from their intensities was about 2000° K. The R_2 lines were not distinguishable in the H_2 and O_2 spectra, and a temperature determination was not possible, but S_{21} line intensities from these spectra have already been shown to give a reasonable rotational temperature. Figure 14 shows the S_{21} line intensities plotted against K from the oxyacetylene flame and a curve plotted from the theoretical data for 3000° K from reference 20. With the experimental curve drawn as shown, a rotational temperature of approximately 2000° K was determined for the outer cone of the oxyacetylene flame, in agreement with the earlier result using the R_2 lines. The spread in data points appears to be ± 5 percent, which is comparable to that used for the combustor data shown previously in figure 12.

The marked difference between the R_2 and S_{21} lines in the two flames can be clearly seen in the spectra. Since the R_2 lines are much more intense, there is apparently more self-absorption in these lines, especially at pressures of 300 pounds per square inch absolute or more. If temperature determinations are to be made, lines of low intensity should be used. Use of lines of low intensity, however, leads to more scatter in the line intensity readings.

The limits of $\pm 400^\circ$ K that were imposed on the rotational temperature because of the scatter in the line intensity readings indicate that a precise determination of combustion gas temperature would be difficult to obtain by this method. The more efficient use of optics as well as the increased resolution of the spectrometer and microphotometer would lead to more precise measurement of the OH lines. These lines, however, can still be appreciably self-absorbed or self-reversed.

When an order of magnitude measurement was taken of the emissivity of the H_2 and O_2 combustion gases, it yielded values varying from 0.022 at 6300 A to 0.388 at 3100 A. These measurements were based on an assumed gas temperature of 3200° K and were determined by means of the calibration technique described in the appendix. An emissivity of 0.388 at 3100 A indicates that appreciable self-absorption is characteristic of the gases (ref. 21). This self-absorption could lead to a distortion of the iso-intensity plot (eq. (4)) and a higher temperature determination than the actual value (ref. 21). Accurate determination of line intensities, therefore, involves additional experimentation to determine the amount of self-absorption.

Determination of OH Line Width

The weak OH lines in the spectra from H_2 and O_2 burning at 300 pounds per square inch absolute appeared to be wider than either the OH lines in the oxyacetylene spectra at atmospheric pressure (fig. 13) or the mercury-calibration lines. This observation suggested that, since the OH lines were sufficiently broadened by pressure, it might be possible to determine the approximate line half-width (the line width at half-intensity) with the relatively low dispersion spectrograph used in this study.

The procedure for determining the line half-width was as follows: With the slits on the spectrograph set at the 20-micron width, the apparent total half-width of the mercury line at 3027.50 A was 0.44 A. Since the calculated Doppler width of the mercury emission line is several orders of magnitude narrower than this, the observed shape was taken to be the slit function of the instrument. The observed OH line (fig. 15), which was recorded with the slits set at 20 microns, was wider

than the actual line because of the error introduced by the slit function. To allow for this error, a gaussian shape and a half-width were assumed as the actual line, and the effect of the slit function was summed at intervals of $\Delta\lambda$ (.11 Å) away from the line center λ_0 . When the actual half-width of the line was assumed to be 0.58 Å, the summation yielded a line shape which closely approximated that of the observed line (fig. 15).

The half-width of 0.58 Å obtained in this manner is considerably greater than that obtained by previous investigators at atmospheric pressure (e.g., 0.014 Å, ref. 22). If this difference is attributable to the difference in pressures, then line broadening due to pressure is substantial.

Other line shapes could have been chosen that would have more closely approximated the actual OH line profile (ref. 21), but the accuracy of the data did not warrant the refinements.

It was shown earlier in this paper that the self-absorption of the intense OH lines was appreciable. Although a weak line was chosen for determining the line width, broadening of this line due to self-absorption was not evaluated.

It must be noted that the location of the spectrometer inside the test cell led to vibration of the components. Diffuse, wide, spectral lines like those shown previously (figs. 3, 4, and 7) resulted, but they are not indicative of line broadening. The spectra used for determining the broadening shown here, however, were obtained in a vibration-free environment, where the spectrometer was located outside the rocket test cell.

Variation of Spectral Intensity with Combustor Run Length

Various run lengths were used to obtain the variation of exposure on the film with time for selected wavelengths (fig. 16). The limited number of points indicates a linear increase in exposure of O_2 and continuum radiation, with the exception of the 2-second run.

In the same series of runs the exposure caused by Na at 5890 and 5896 Å decreased as the run length increased (fig. 17). The data were obtained from four consecutive runs with no change in the hardware or the ignition plug. When the hardware and the ignition plug were replaced or cleaned between runs, exposure because of the Na lines increased with run length. This behavior indicated that sodium was a contaminant in the system.

The important consideration appeared to be the elapsed running time on the ignition plug, which led to the outgassing of the contaminants (i.e., sodium). Since there was evidence of wear and cracks in the ceramic surface after several runs, it is believed that the contaminants were present in the ceramic portion of the sparkplug.

SUMMARY OF RESULTS

Emission spectra were obtained from a nominal 200-pound-thrust hydrogen-oxygen combustor for the wavelength range 2100 to 7800 Å. Radiation consisted of the hydroxyl (OH) bands from 2444 to 3546 Å, the Schumann-Runge oxygen (O₂) emission from 2400 to 4600 Å, the sodium D lines at 5890 and 5896 Å, and a continuum extending throughout the sensitivity range of the film.

Intensities of the OH lines, the O₂ lines, and the continuum varied with the pressure as p^n , where n varied for the continuum from 3.2 to 2.4 over the pressure range 150 to 450 pounds per square inch absolute and for O₂ from 2.6 to 2.0 over the pressure range 150 to 325 pounds per square inch absolute.

The increase in line intensities with oxidant-fuel weight ratio was small compared to the variation expected from thermochemical equilibrium calculations. When it was assumed that the radiation originated in regions that had a statistical distribution of oxidant-fuel mixtures, good agreement was achieved between the experimental and theoretical results. These results indicate that the combustion gases were undergoing various degrees of reaction with a wide distribution in gas temperature and composition. It appears, therefore, that statistical techniques might be advantageously used in the study of rocket combustion.

The rotational temperature of the rocket combustor gases was $3250^\circ \pm 400^\circ$ K, which is in reasonable agreement with the theoretical temperature of 3560° K. This temperature was determined from an iso-intensity plot of the S₂₁ lines of the O, O transition of OH. No temperature determinations were possible from the other branches of the same transition because of the severe self-absorption and self-reversal of the lines.

In order to obtain the actual line width, the width of an OH line in the spectra from the combustor was compared with that of a mercury line in the same spectral region. A gaussian half-width of 0.58 Å was derived from the observed lines. This half-width was more than 40 times greater than the half-widths cited in the literature for OH lines in spectra at 1 atmosphere. These findings indicate a substantial broadening of the lines on account of pressure.

Exposure on the film caused by the O_2 and the continuum radiation increased linearly with run time, while exposures caused by the sodium lines decreased with run time. As long as combustor hardware was not changed, the same results were obtained. Hence, sodium must have been a contaminant in the combustor components.

Lewis Research Center

National Aeronautics and Space Administration
Cleveland, Ohio, April 12, 1962.

E-1621

APPENDIX - INTENSITY CALIBRATION OF FILM

E-1621

A tungsten-ribbon - filament lamp calibrated by the National Bureau of Standards was used to obtain a calibration on each type of film. Eight current settings were used to obtain the spectra. Each spectrum was scanned by a recording microphotometer to obtain curves of transmission against wavelength. One of these curves is shown in figure 18. Intensity-wavelength data were supplied with the lamp for two current settings, and data for the other current settings were obtained by measuring the apparent filament temperatures, converting them to true temperatures, and using Planck's Law with emissivity data supplied with the lamp.

Comparison of the transmission-wavelength data and intensity-wavelength data yielded a curve of transmission against intensity at each wavelength. The slopes of these transmission-intensity curves were nearly the same; therefore, they coincided reasonably well with a single curve if a multiplying factor for film sensitivity was used for each wavelength (figs. 19 and 20).

REFERENCES

1. Gaydon, A. G., and Wolfhard, H. G.: Predissociation in the Spectrum of OH; the Vibrational and Rotational Intensity Distribution in Flames. Proc. Roy. Soc., ser. A, vol. 208, no. A1092, Aug. 7, 1951, pp. 63-75.
2. Broida, Herbert P.: Rotational Temperatures of OH in Methane-Air Flames, Jour. Chem. Phys., vol. 19, no. 11, Nov. 1951, pp. 1383-1390.
3. Penner, S. S., Gilbert, M., and Weber, D.: Spectroscopic Studies of Low Pressure Combustion Flames. Jour. Chem. Phys., vol. 20, no. 3, Mar. 1952, pp. 522-523.
4. Broida, H. P., and Ialos, G. T.: Rotational Temperatures of OH in Several Flames. Jour. Chem. Phys., vol. 20, no. 9, Sept. 1952, pp. 1466-1471.
5. Kane, W. R., and Broida, H. P.: Rotational "Temperatures" of OH in Diluted Flames. Jour. Chem. Phys., vol. 21, no. 2, Feb. 1953, pp. 347-354.
6. Broida, Herbert P., and Kostkowski, Henry J.: Experimental Evidence for the Existence of Abnormal OH Rotational "Temperatures" in Low-Pressure Flames. Jour. Chem. Phys., vol. 23, no. 4, Apr. 1955, p. 754.

7. Broida, Herbert P., and Heath, Donald F.: Spectroscopic Survey of Energy Distributions of OH, C₂, and CH Radicals in Low Pressure Acetylene-Oxygen Flames. Jour. Chem. Phys., vol. 26, no. 2, Feb. 1957, pp. 223-229.
8. Wolfhard, H. G., and Parker, W. G.: A Spectroscopic Investigation into the Structure of Diffusion Flames. Proc. Phys. Soc., sec. A, vol. 65, no. 385A, Jan. 1952, pp. 2-19.
9. Kitagawa, T.: Formation of Activated Water Molecules in High Vibrational States in the Oxy-hydrogen Flame. Proc. Imp. Acad. Tokyo, vol. 12, 1936, pp. 281-284.
10. Gaydon, A. G.: Spectroscopy and Combustion Theory. Second ed. Chapman and Hall (London) 1948.
11. Gaydon, A. G.: The Spectroscopy of Flames. John Wiley & Sons, Inc. 1957.
12. Liveing, G. D., and Dewar, J.: On the Influence of Pressure on the Spectra of Flames. Proc. Roy. Soc., ser. A, vol. 49, 1891, p. 217.
13. Kaskan, Walter E.: Abnormal Excitation of OH in H₂/O₂/N₂ Flames. Jour. Chem. Phys., vol. 31, no. 4, Oct. 1959, pp. 944-956.
14. Auble, Carmon M., and Heidmann, Marcus F.: The Application of Radiation Measurement Techniques to the Determination of Gas Temperatures in Liquid Propellant Flames. Jet Prop., pt. 1, vol. 25, no. 9, Sept. 1955, pp. 449-453; con't., p. 467.
15. Heidmann, M. F., and Priem, R. J.: Application of an Electro-Optical Two-Color Pyrometer to Measurement of Flame Temperature for Liquid Oxygen - Hydrocarbon Propellant Combination. NACA TN 3033, 1953.
16. Hersch, Martin: Determinations of Local and Instantaneous Combustion Conditions from Acoustic Measurements in a Rocket Combustor and Comparison with Overall Performance. NASA TN D-1192, 1962.
17. Summerfield, Martin, Reiter, Sydney H., Kebely, Victor, and Mascolo, Richard W.: The Physical Structure of Turbulent Flames. Jet Prop., vol. 24, no. 4, July-Aug. 1954, pp. 254-255.
18. Povinelli, L. A.: A Review of Turbulent Flame Propagation. L'Aerotecnica (Rome), vol. XL, no. 5, Oct. 1960, pp. 272-286.

- E-1621
19. Povinelli, L. A., and Fuhs, A. E.: The Spectral Theory of Turbulent Flame Propagation. Eighth Symposium (International) on Combustion, The Williams & Wilkins Co., 1962, pp. 554-566.
 20. Dieke, G. H., and Crosswhite, H. M.: The Ultra Violet Bands of OH - Fundamental Data. Bublebee Rep. 87, Appl. Phys. Lab., Johns Hopkins Univ., Nov. 1948.
 21. Penner, S. S.: Quantitative Molecular Spectroscopy and Gas Emissivities. Addison-Wesley Pub., 1959.
 22. Carrington, Tucker: Line Shape and f Value in the $\text{OH}^2\Sigma^+ - 2\pi$ Transition. Jour. Chem. Phys., vol. 31, no. 5, Nov. 1959, pp. 1243-1252.
 23. Physics and Mathematics Unit: Tables for the Spectral Radiant Intensity of a Blackbody and of a Tungsten Ribbon. Rep. 59-32, Rocketdyne Co., 1959.

TABLE I. - RADIATION INTENSITY CALCULATIONS

Oxidant-fuel weight ratio, o/f	Mole fraction, n	$k_{\lambda} n I_P$	Emissivity, ϵ_{λ}	Temperature, T , $^{\circ}K$	Black-body radiation intensity, I_{BB} , (w) (cm^{-2}) (micron $^{-1}$) (steradian $^{-1}$) (b)	Radiation intensity, I , (w) (cm^{-2}) (micron $^{-1}$) (steradian $^{-1}$) (c)
(a)						
OH emission; $k_{\lambda} = 0.064 \text{ (cm}^{-1}\text{) (atm}^{-1}\text{)}$						
4	0.011	0.070	0.0675	3073	3.47	00.234
6	.063	.400	.336	3438	14.64	4.92
8	.109	.632	.525	3499	17.97	9.43
10	.125	.795	.580	3453	15.16	8.80
O_2 emission; $k_{\lambda} = 0.096 \text{ (cm}^{-1}\text{) (atm}^{-1}\text{)}$						
4	0.0002	0.00192	0.0032	3073	4.37	00.014
6	.008	.0766	.0716	3438	17.73	1.27
8	.043	.4120	.337	3499	21.63	7.30
10	.102	.9770	.698	3453	18.33	12.80

$a \epsilon_{\lambda} = 1 - e^{-k_{\lambda} n I_P}$, where L is 5 cm and P is 20 atm.

^bRef. 23.

^c $I = \epsilon_{\lambda} I_{BB}$.

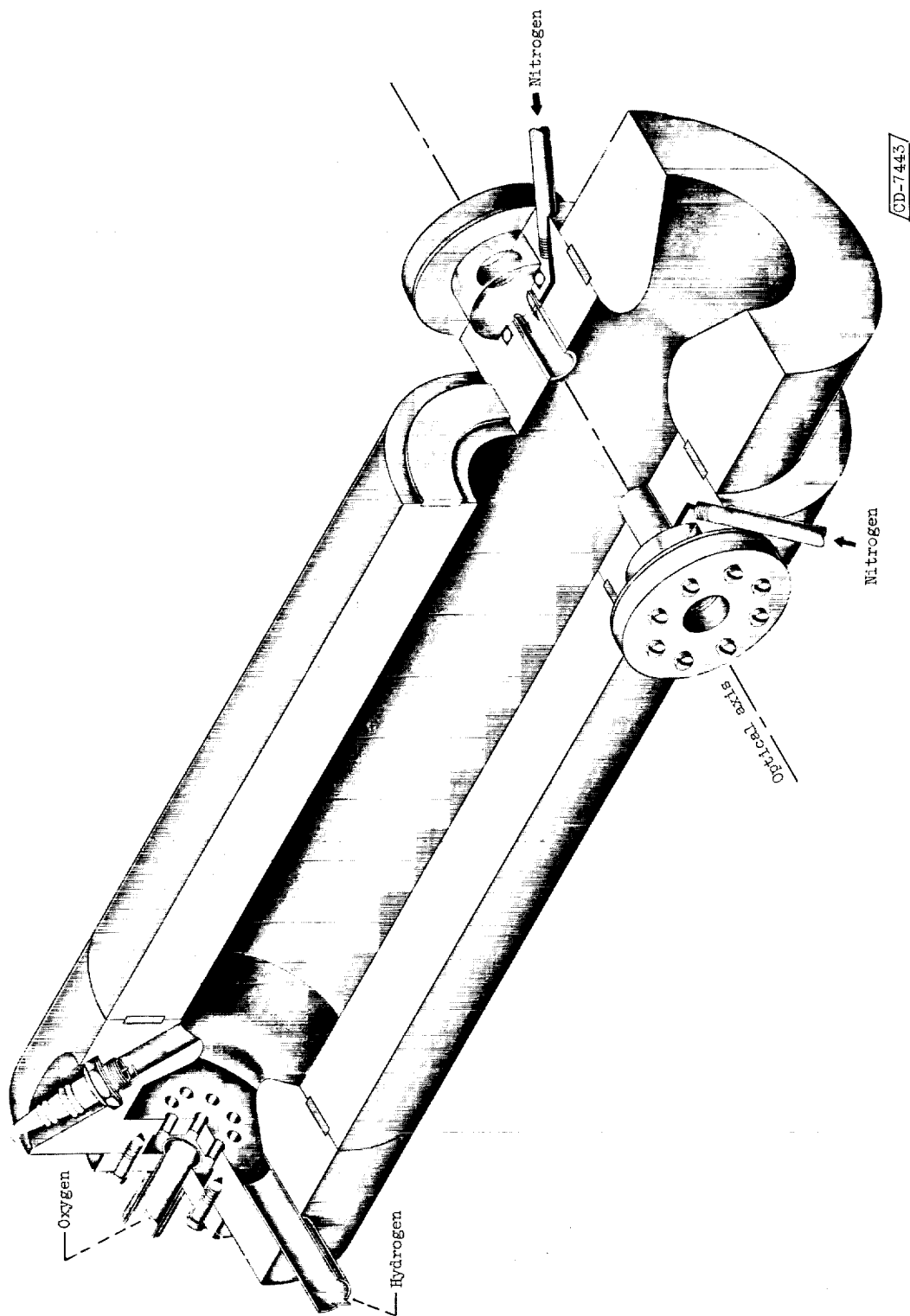


Figure 1. - Gaseous-hydrogen - gaseous-oxygen combustor. Distance from injector to optical axis, 10 inches; chamber diameter, 2 inches; nozzle diameter, 0.658 inch.

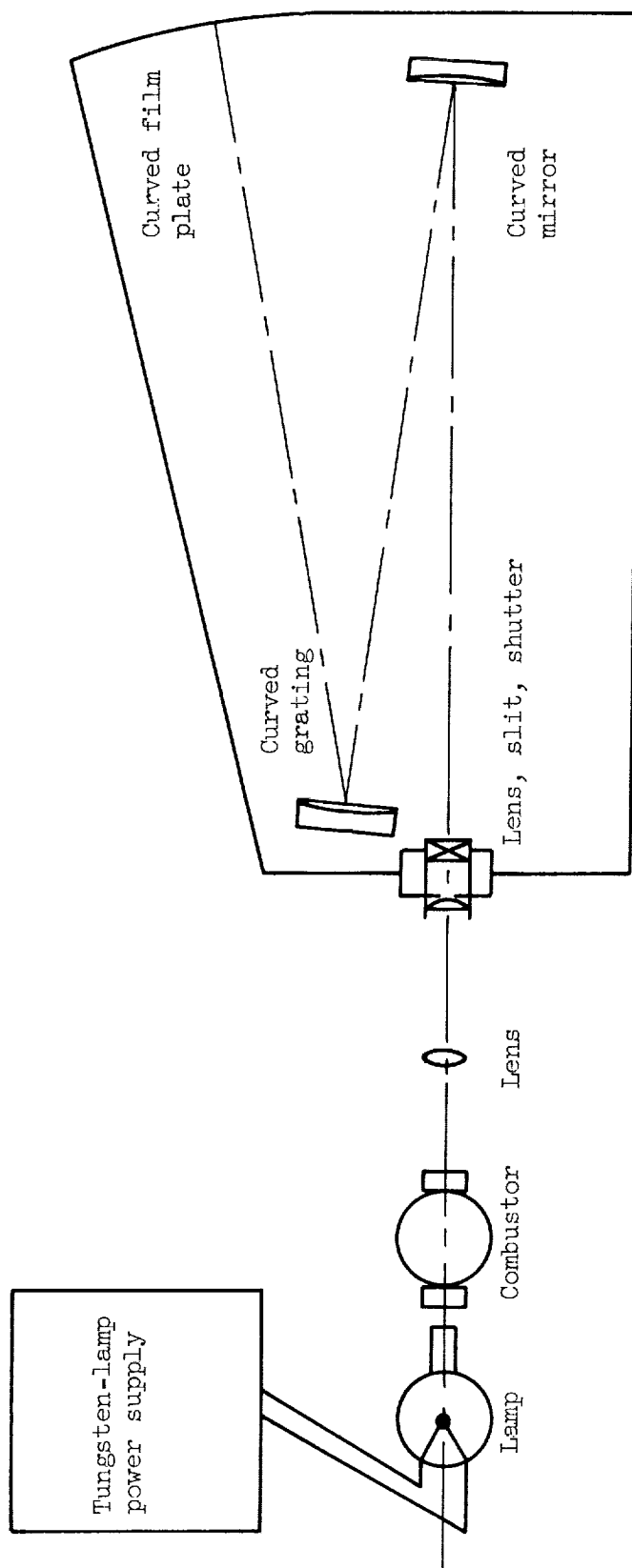
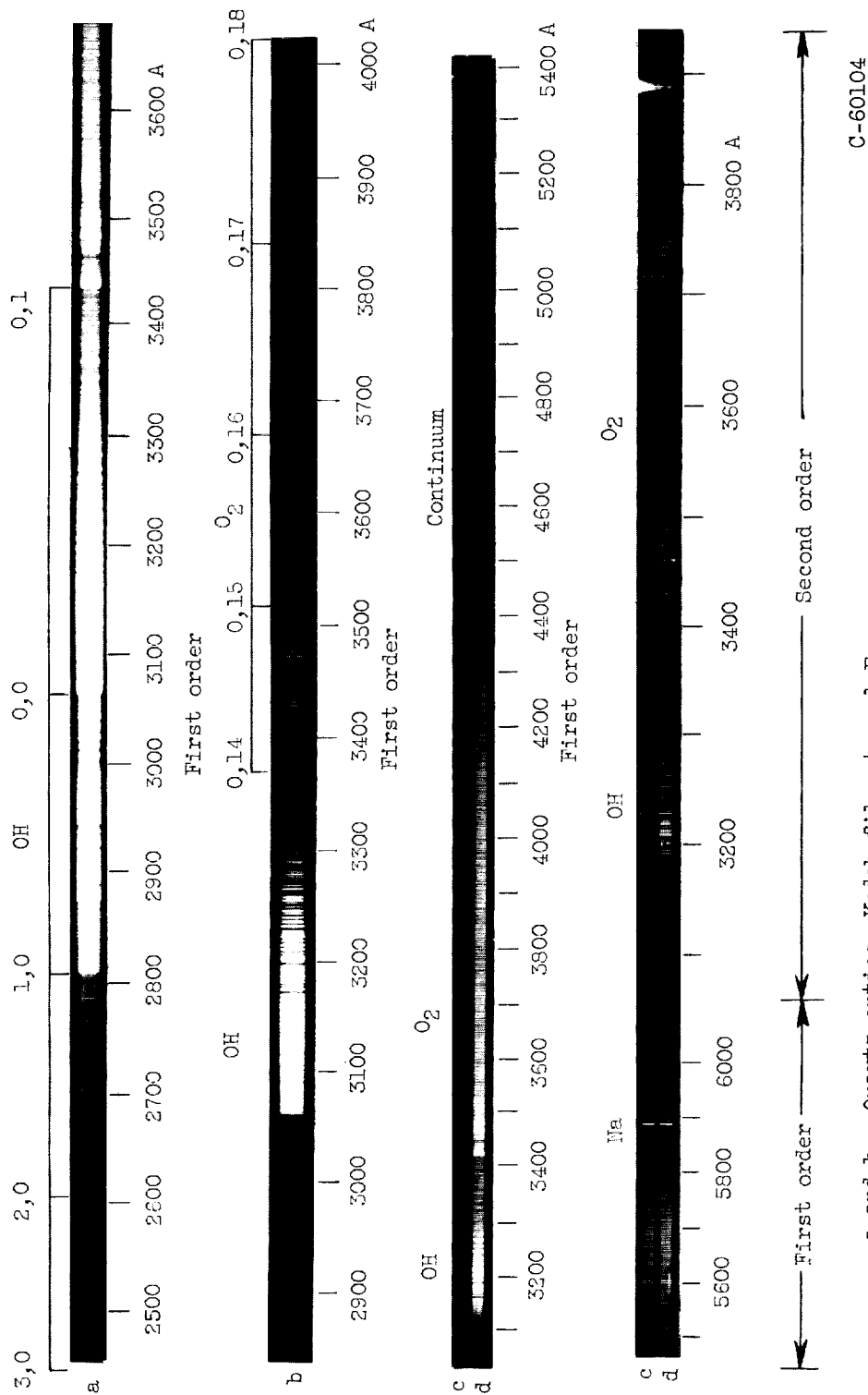


Figure 2. - Schematic diagram of experimental apparatus.



a and b - Quartz optics; Kodak film, type 1-F
 c - Glass optics; Eastman Tri-X film; type 5233; radiation filtered
 by Wratten No. 8 filter to eliminate second-order radiation
 d - Glass optics; Eastman Tri-X film, type 5233; no filter

Figure 3. - Short- and long-wavelength characteristics of hydrogen-oxygen flame radiation. Total weight flow, 0.43 ± 0.02 pound per second; oxidant-fuel weight ratio, 7.4; chamber pressure, 320 ± 15 pounds per square inch absolute; run duration, 2 seconds.

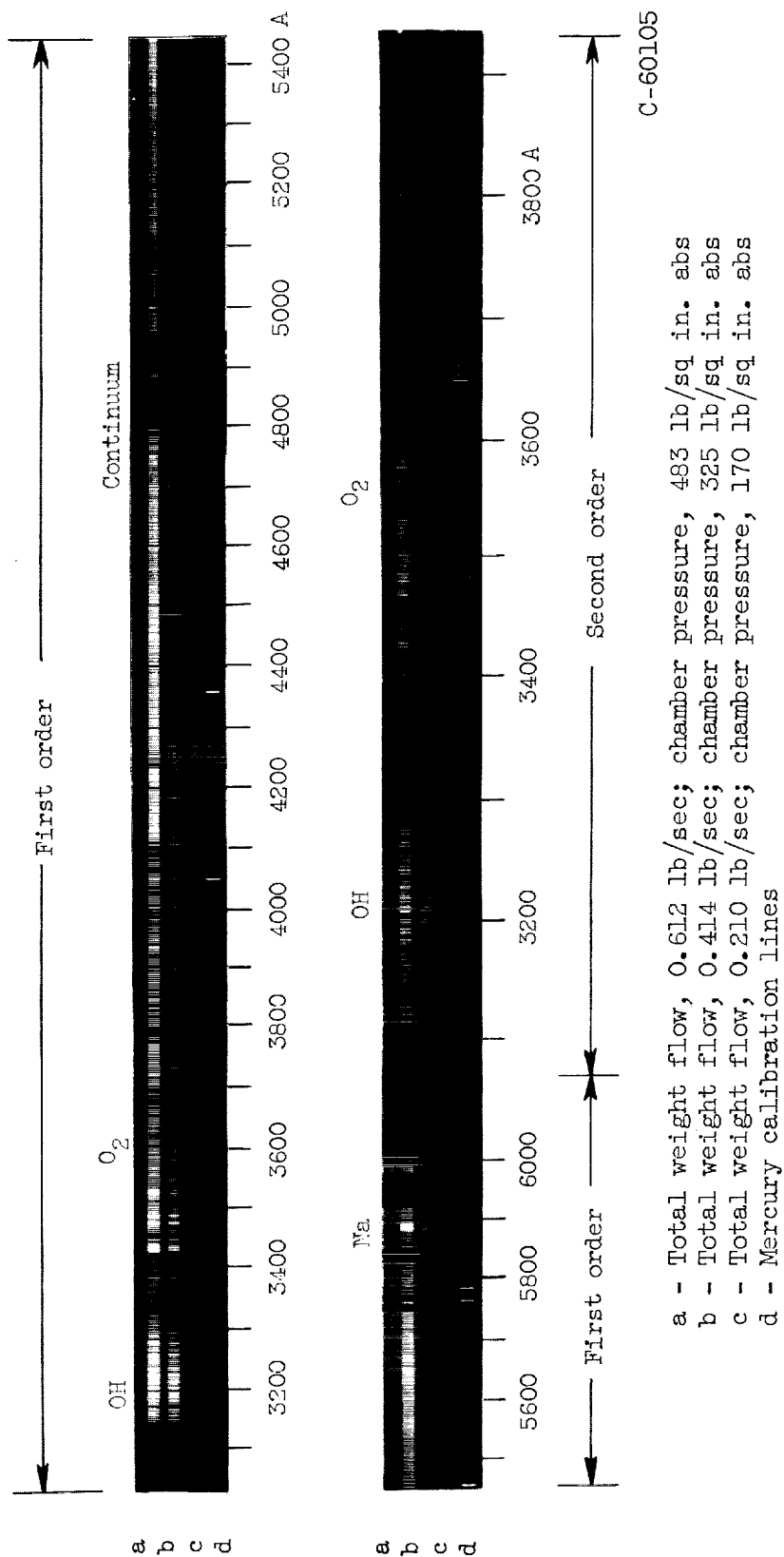


Figure 4. - Variation of spectral intensity with chamber pressure and total weight flow. Oxidant-fuel weight ratio, 4.35±0.11; Eastman Tri-X film, type 5233; glass optics; run duration, 2 seconds.

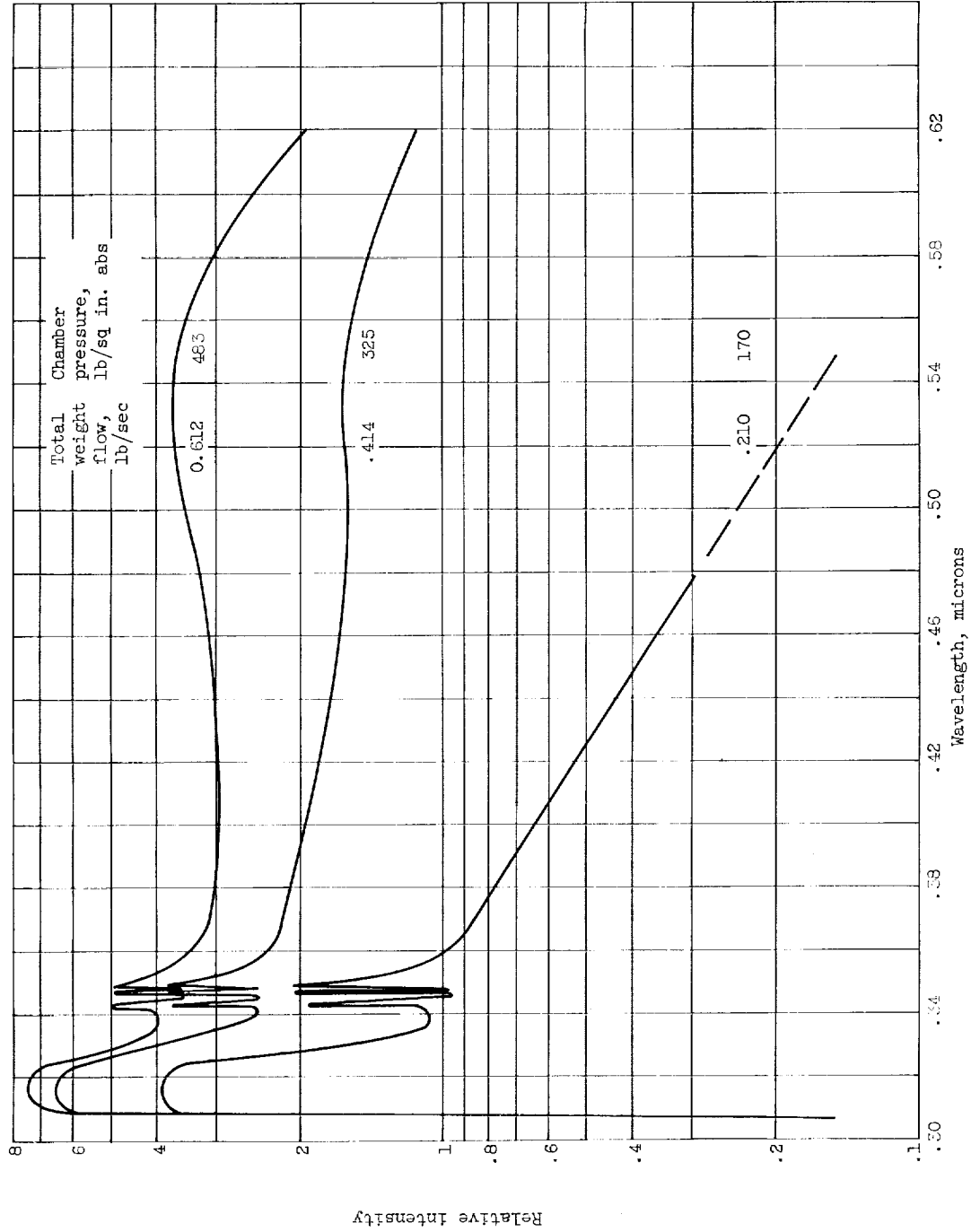


Figure 5. - Variation of spectral intensity with total weight flow and pressure. Intensities accurate to ± 20 percent; oxidant-fuel weight ratio, 4.35 ± 0.11 .

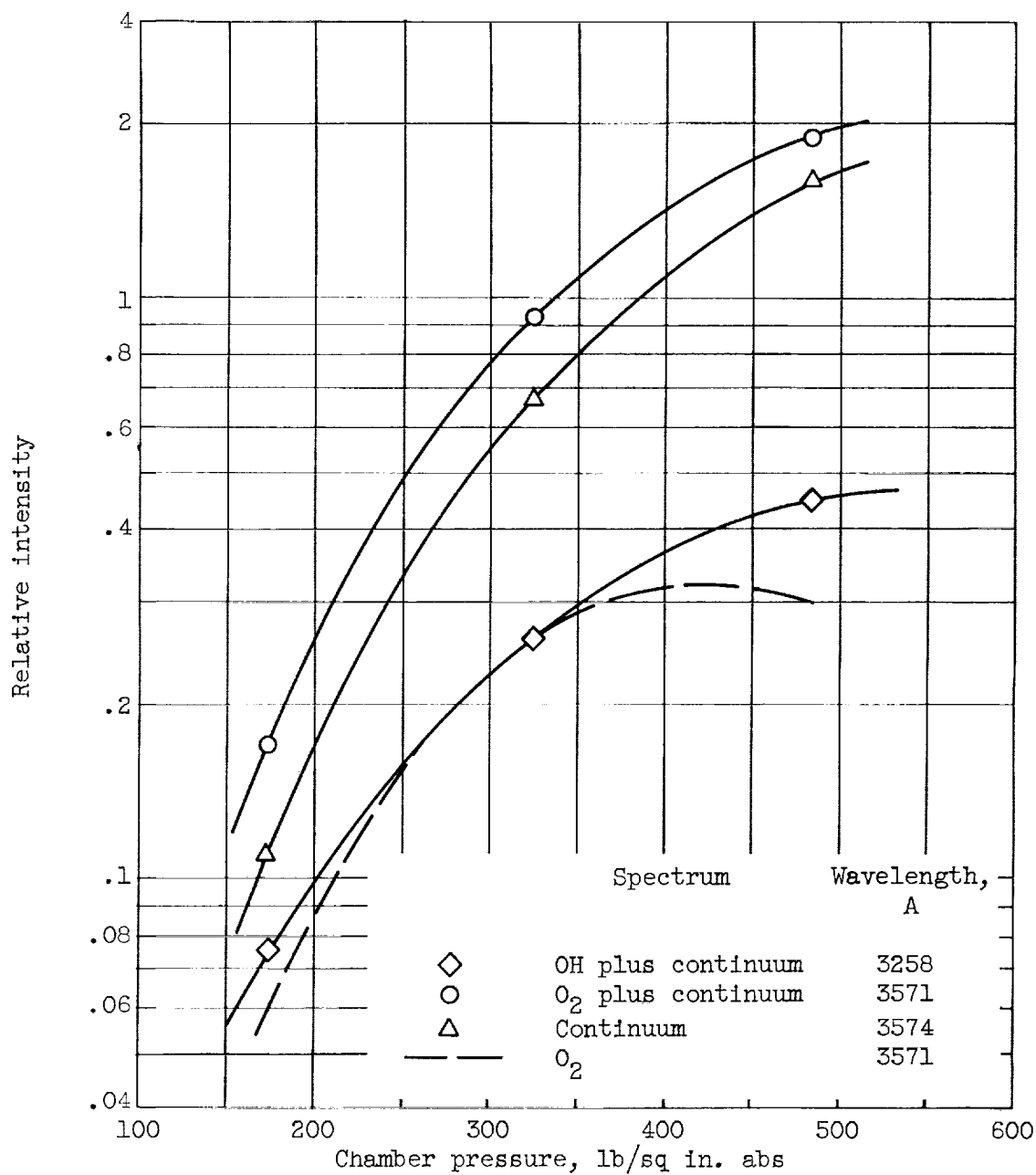


Figure 6. - Spectral radiation intensity as function of rocket chamber pressure. Oxidant-fuel weight ratio, 4.4 ± 0.1 .

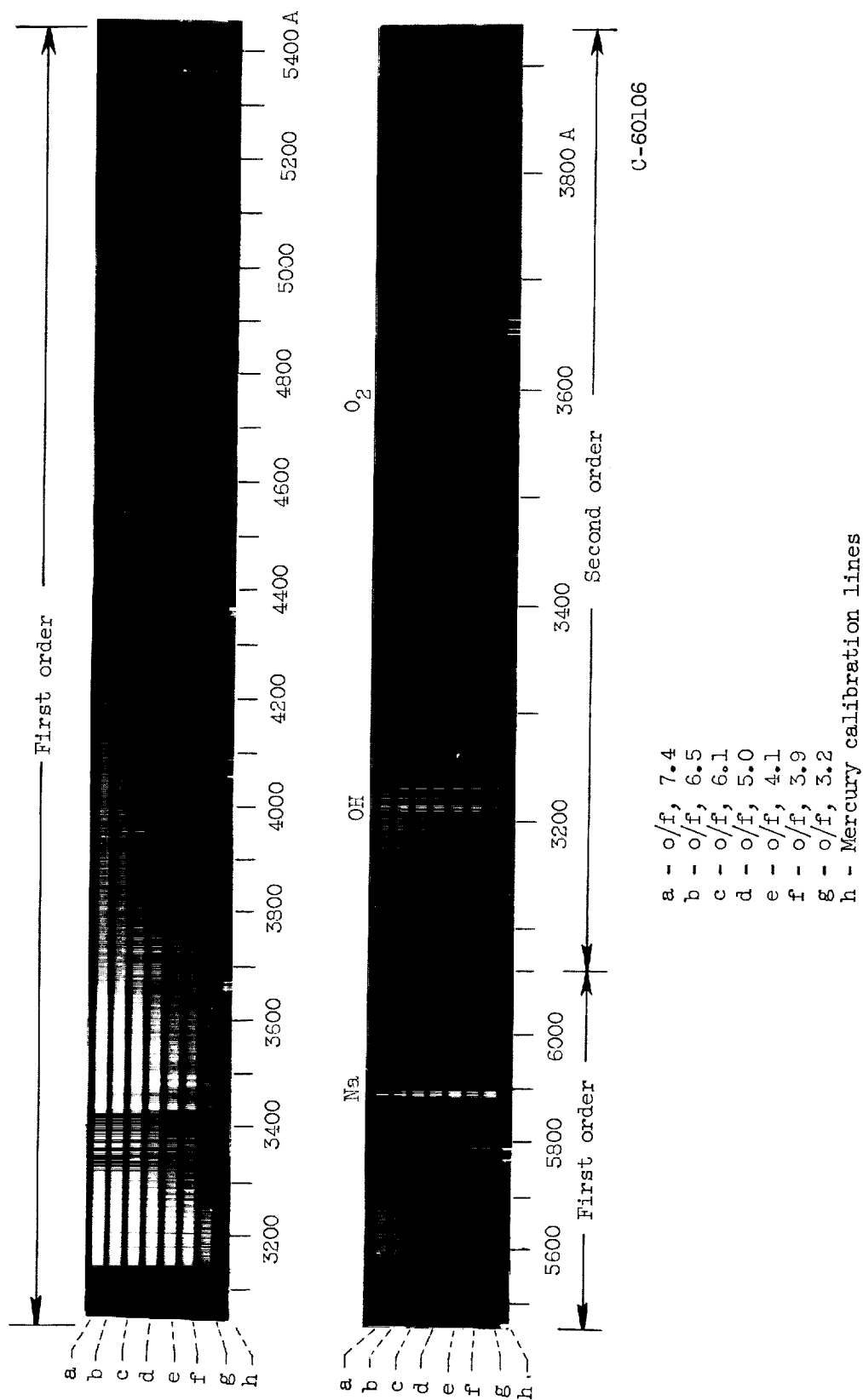


Figure 7. - Variation of spectral intensity with oxidant-fuel weight ratio (o/f). Total weight flow, 0.43 ± 0.02 pound per second; chamber pressure, 320 ± 15 pounds per square inch absolute; Eastman Tri-X film, type 5233; glass optics; run duration, 2 seconds.

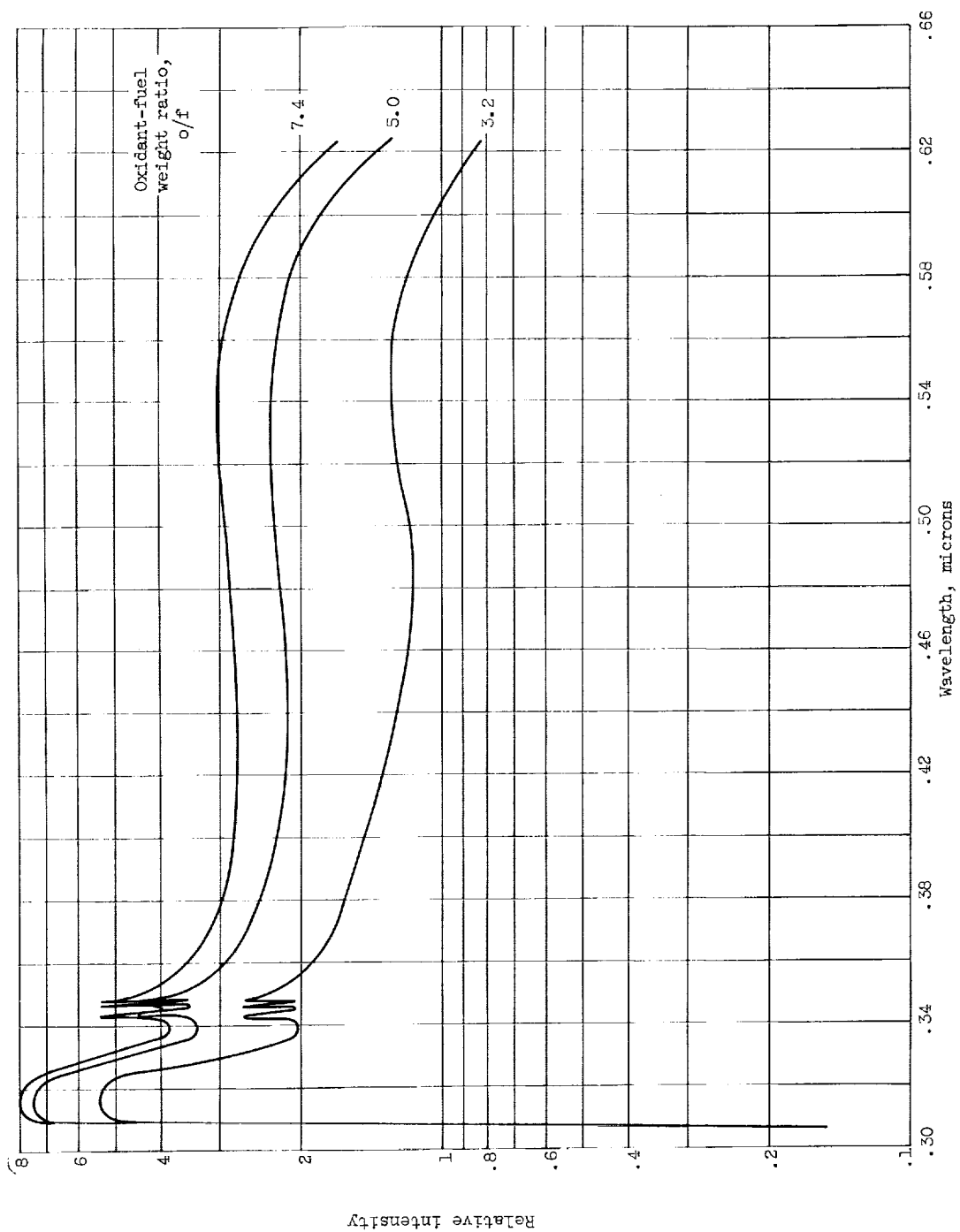


Figure 8. - Variation of spectral intensity with oxidant-fuel ratio. Intensities accurate to ± 20 percent; total weight flow, 0.430 ± 0.024 pound per second; chamber pressure, 320 ± 15 pounds per square inch absolute.

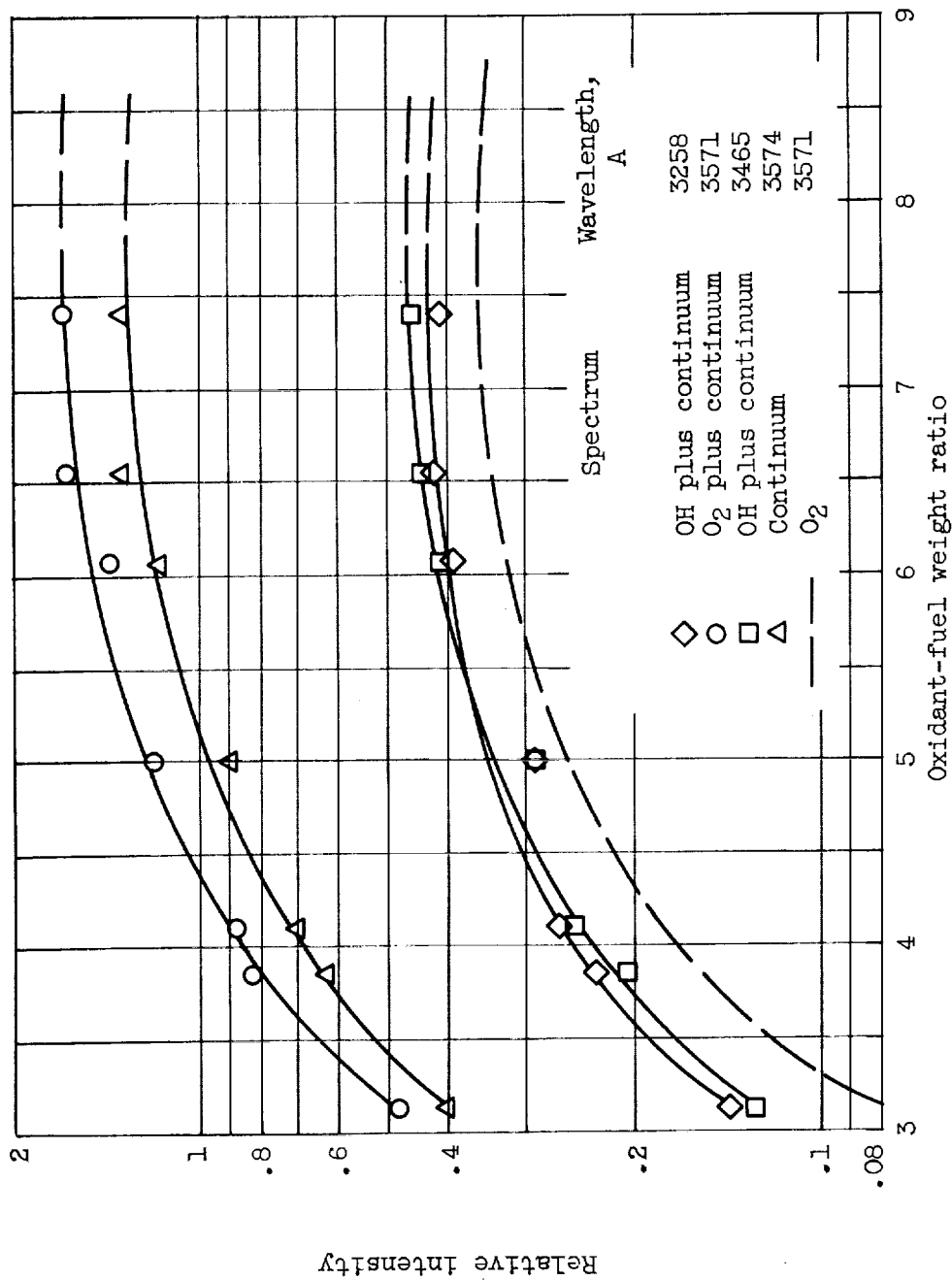


Figure 9. - Spectral radiation intensity as a function of oxidant-fuel weight ratio.

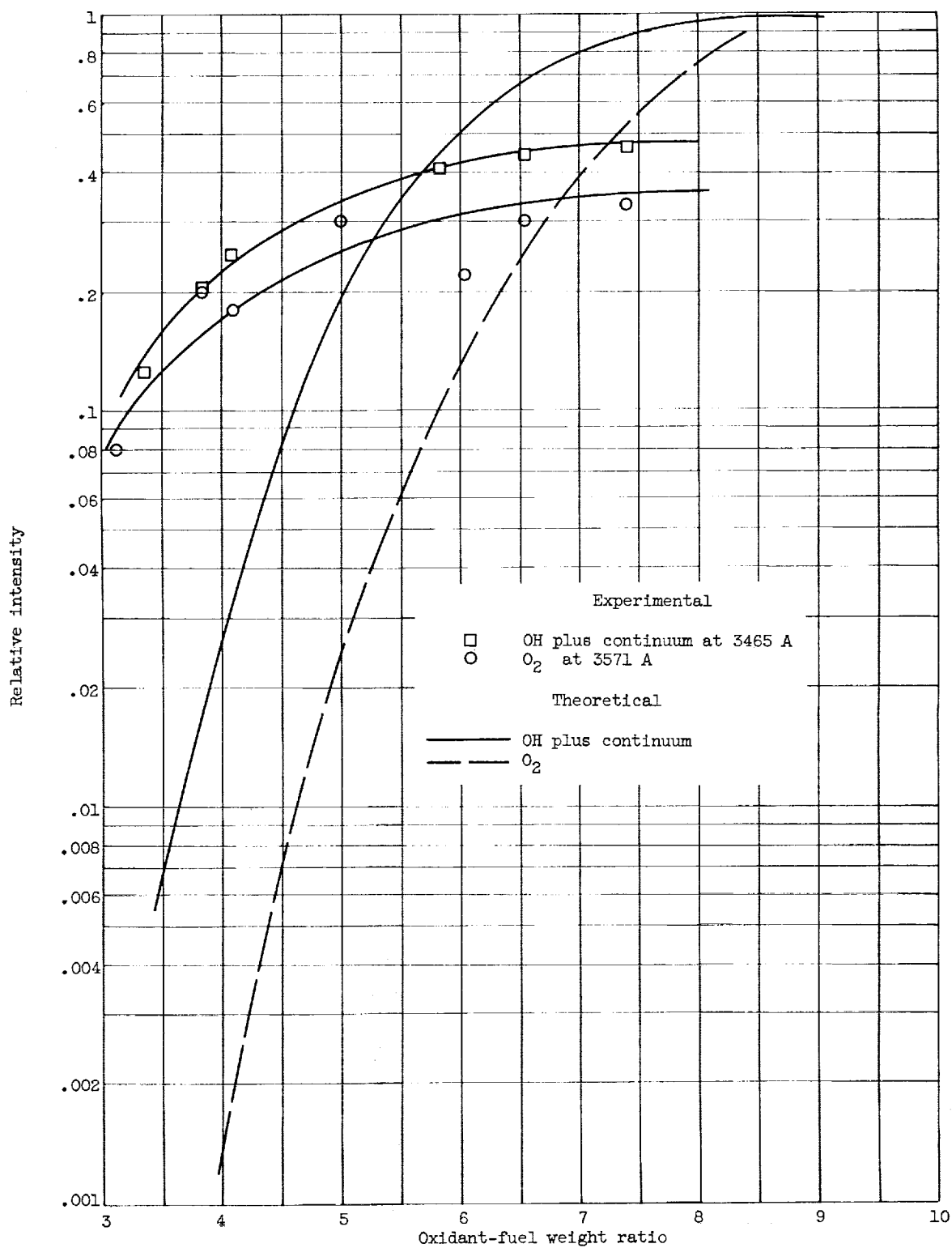
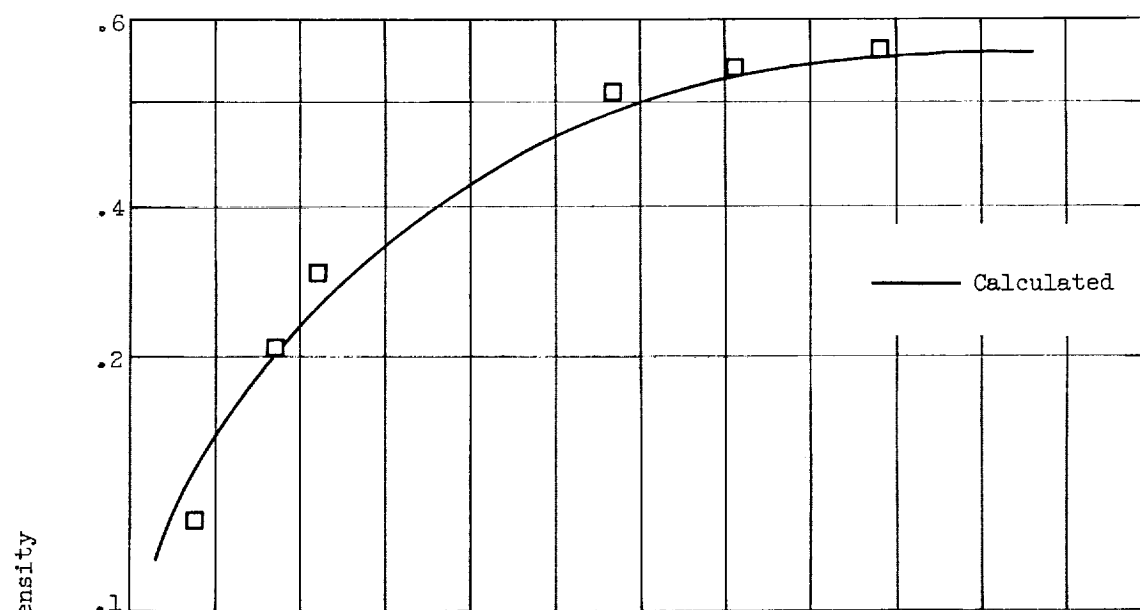


Figure 10. - Comparison of experimental and theoretical data based on Beer-Lambert Law.

E-1621



(a) OH plus continuum at 3465 Å.

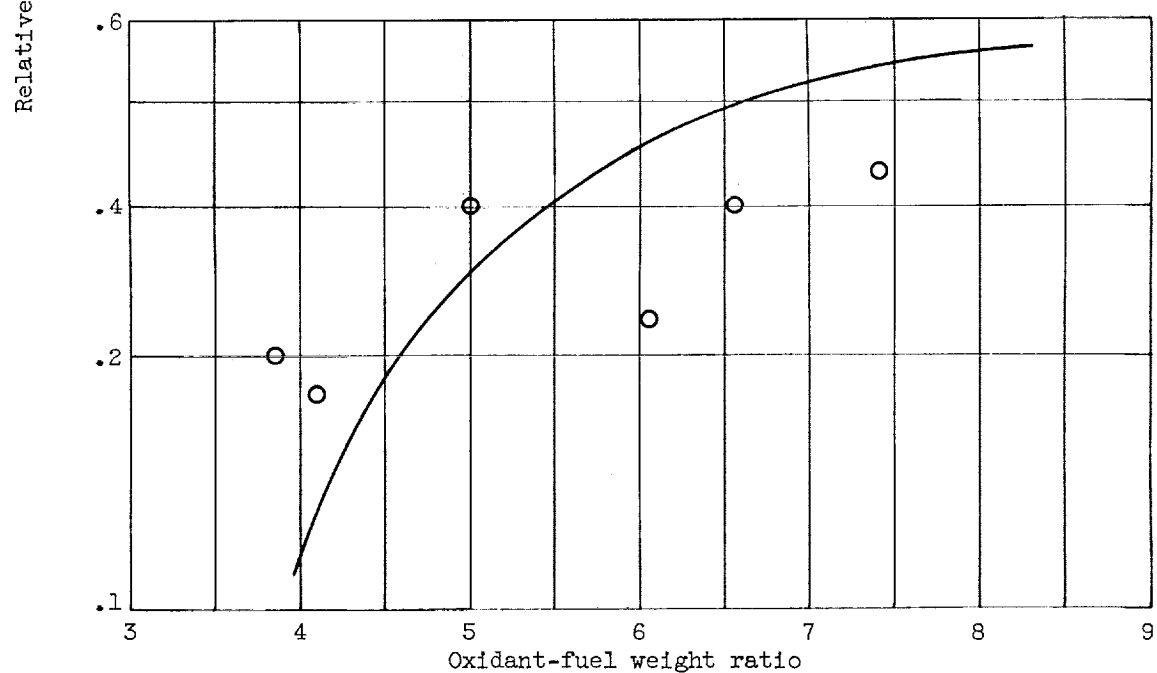
(b) O_2 at 3571 Å.

Figure 11. - Comparison of experimental points and calculated curves based on Beer-Lambert Law (eq. (1)) and log-normal distribution (eq. (2)).

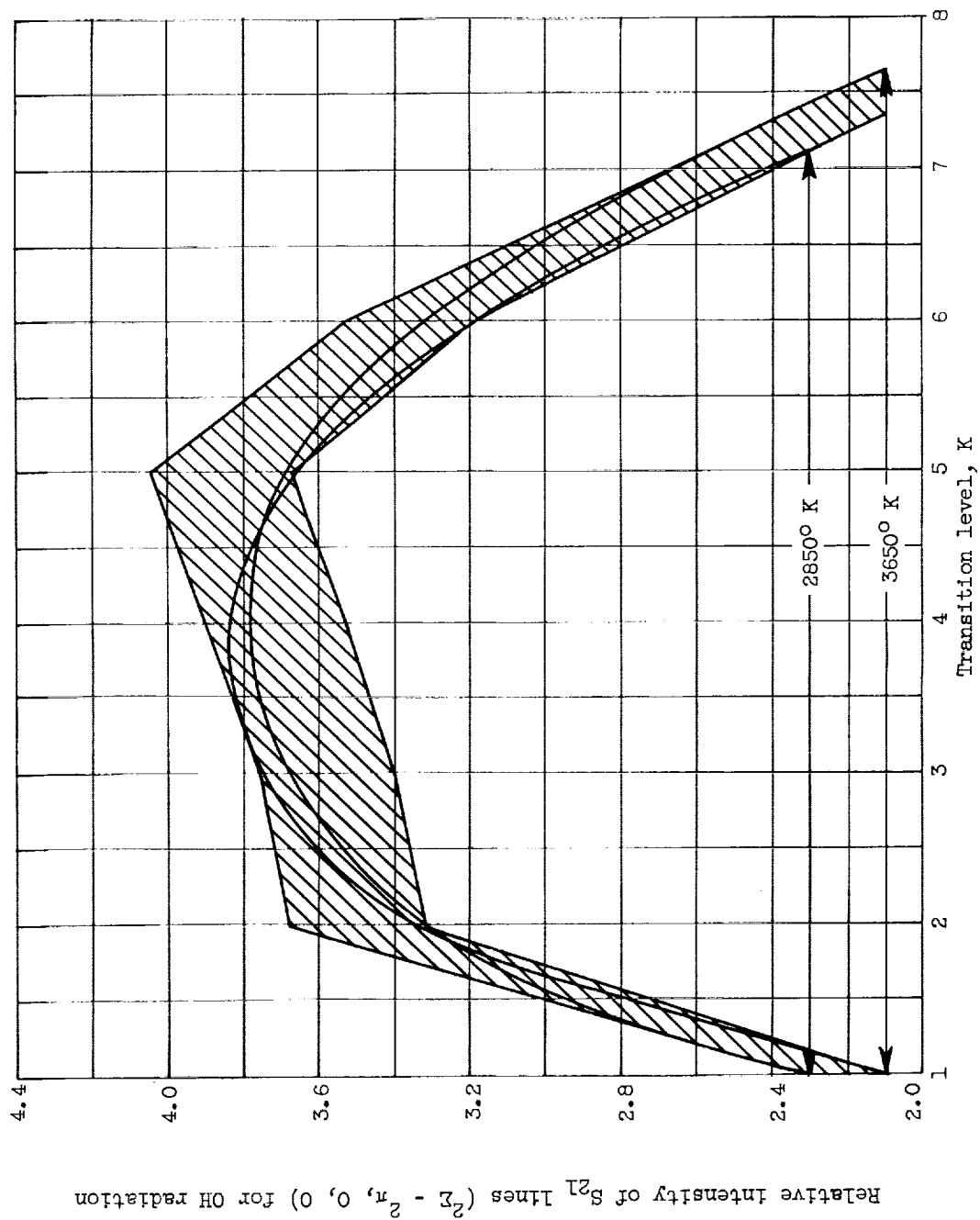
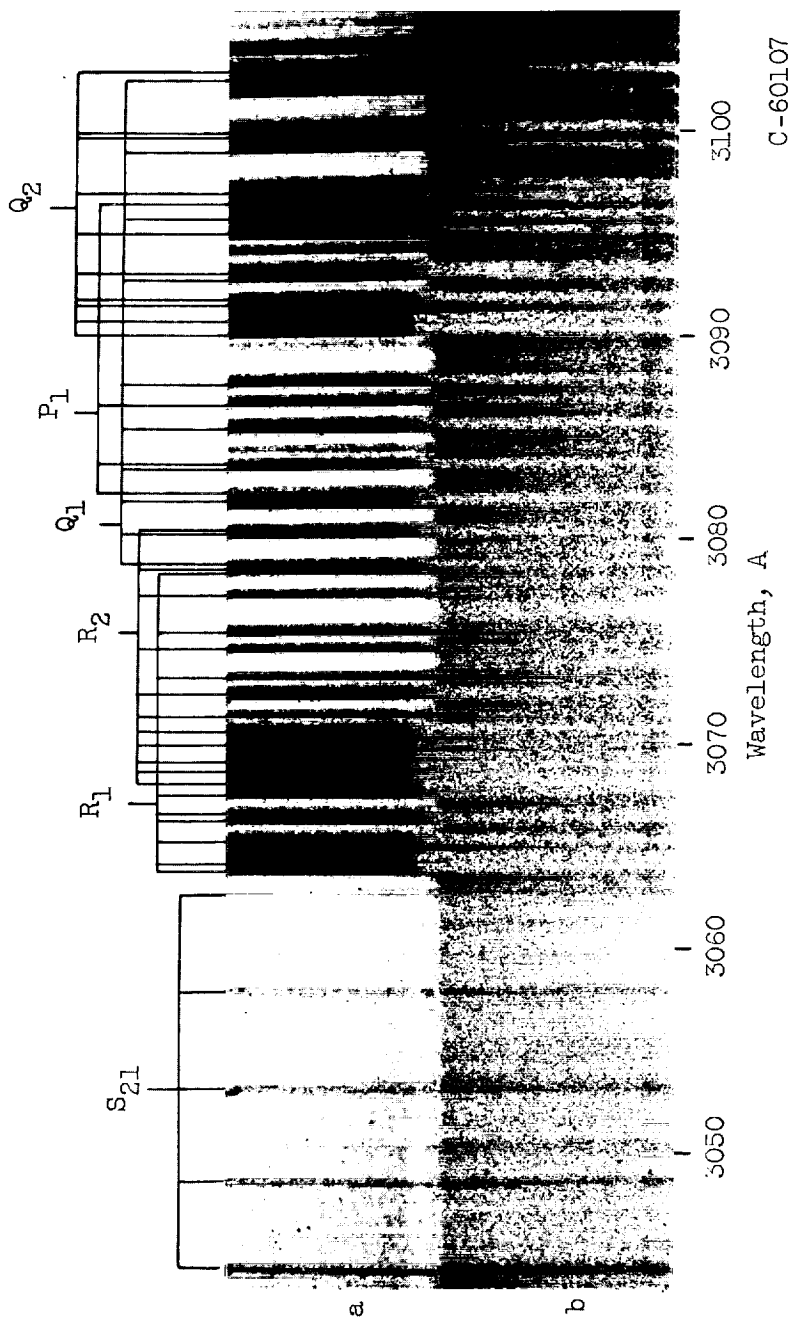


Figure 12. - Isointensity plot of rocket combustion. Chamber pressure, 315 pounds per square inch absolute; temperature, $3250^\circ \pm 400^\circ \text{ K}$.



a - Outer cone of oxyacetylene flame at 1 atm; 75-micron slit; run duration, 300 sec

b - Hydrogen-oxygen flame in rocket combustor; total weight flow, 0.41 lb/sec; chamber pressure, 325 lb/sq in. abs; oxidant-fuel weight ratio, 7.4; 10-micron slit; run duration, 4 sec

Figure 13. - Self-reversal in ($^2\Sigma - ^2\pi$, 0, 0) OH band. Second order spectra; Kodak spectroscopic film, type 1-F.

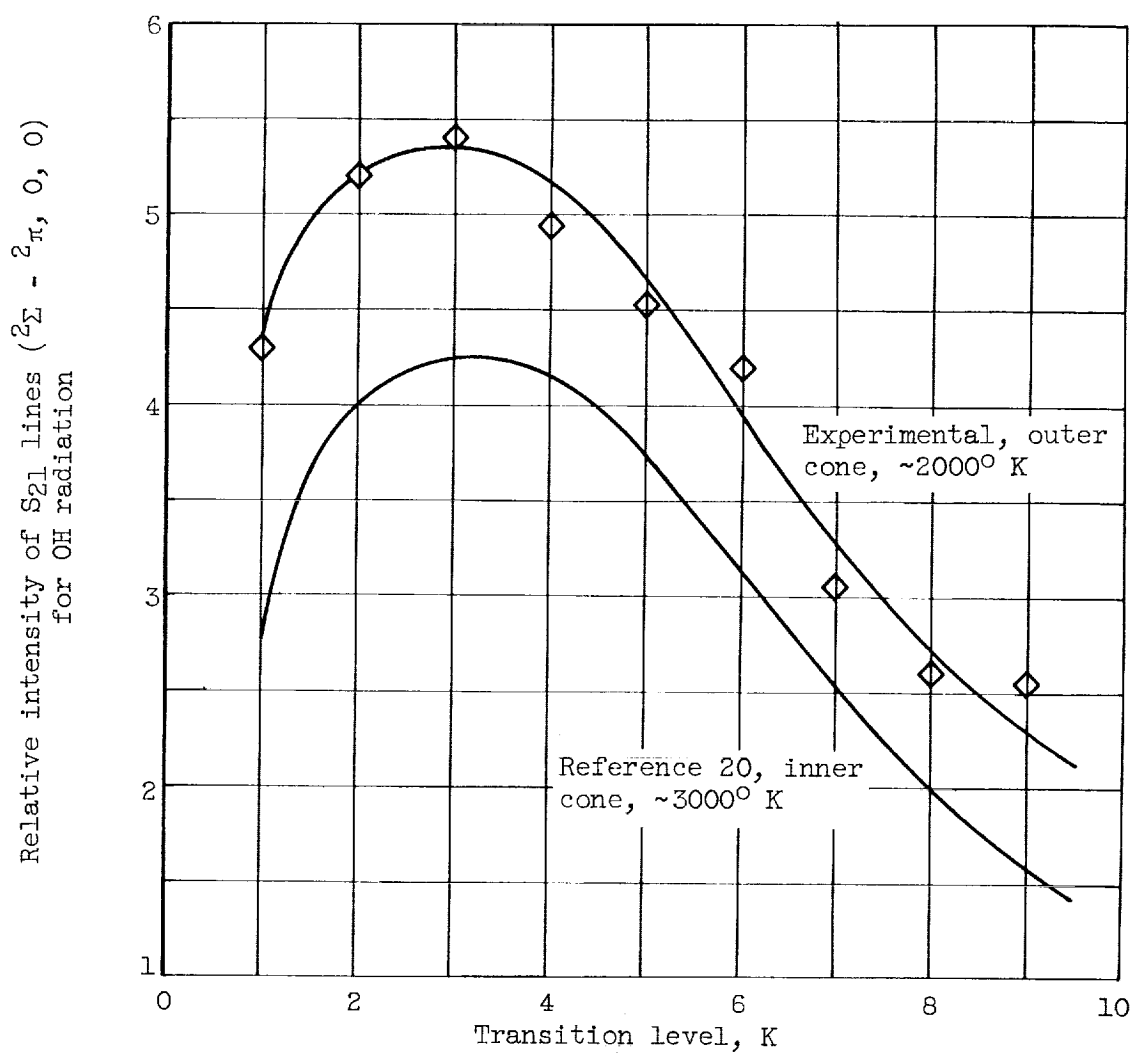


Figure 14. - Isointensity plot of oxyacetylene-atmospheric flames.

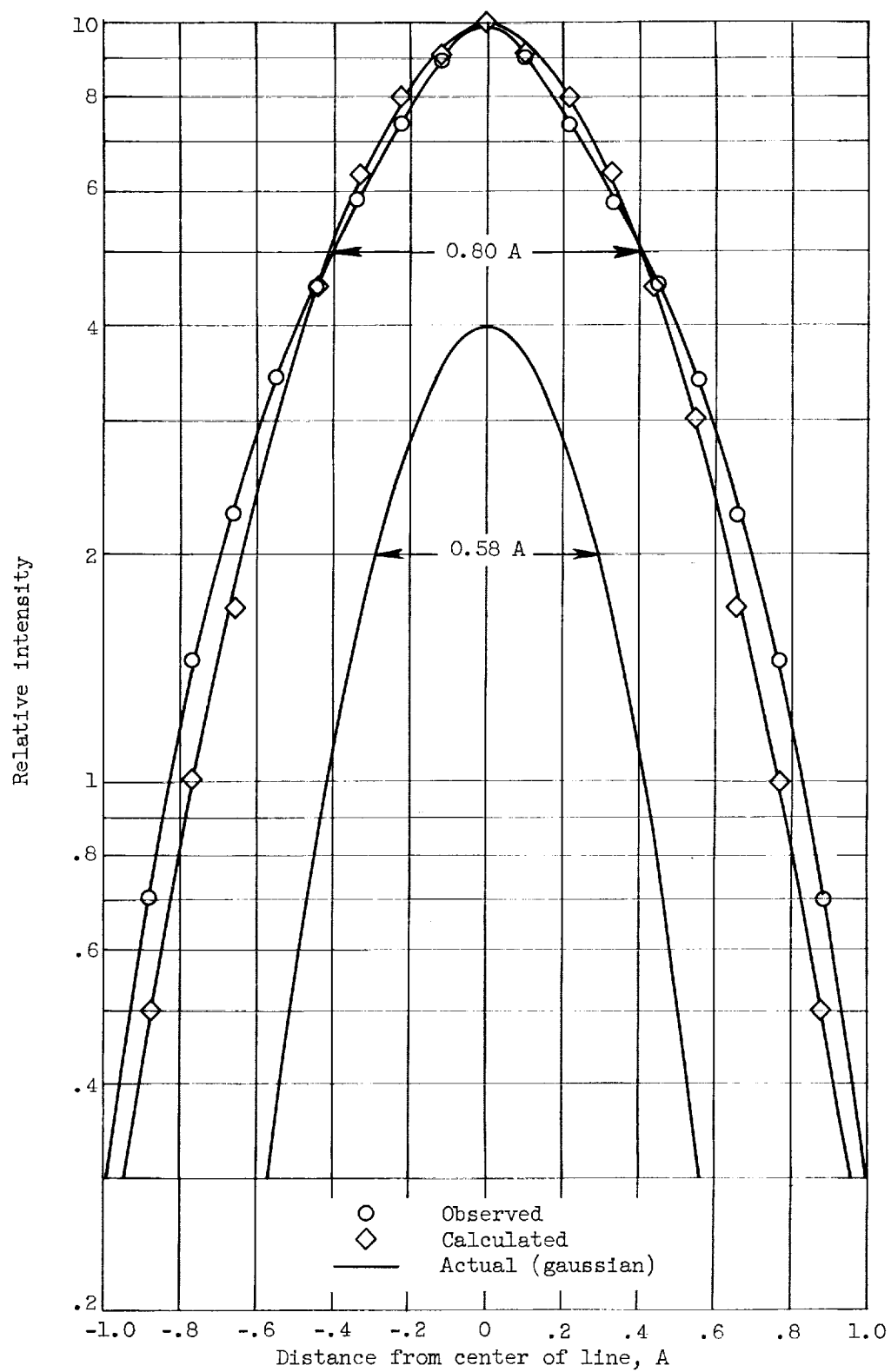


Figure 15. - OH line profiles. Center of OH line, 3048.565 A.

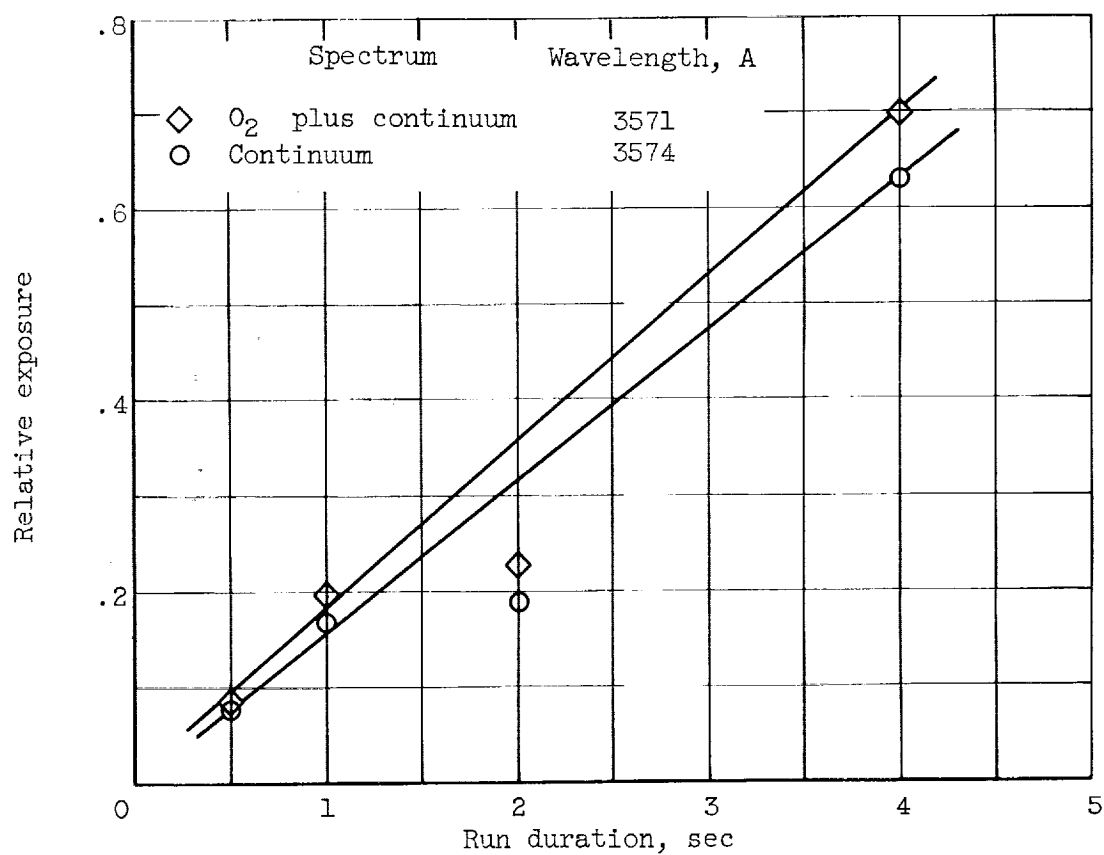


Figure 16. - Oxygen-continuum emission as a function of combustion time.

E-1621

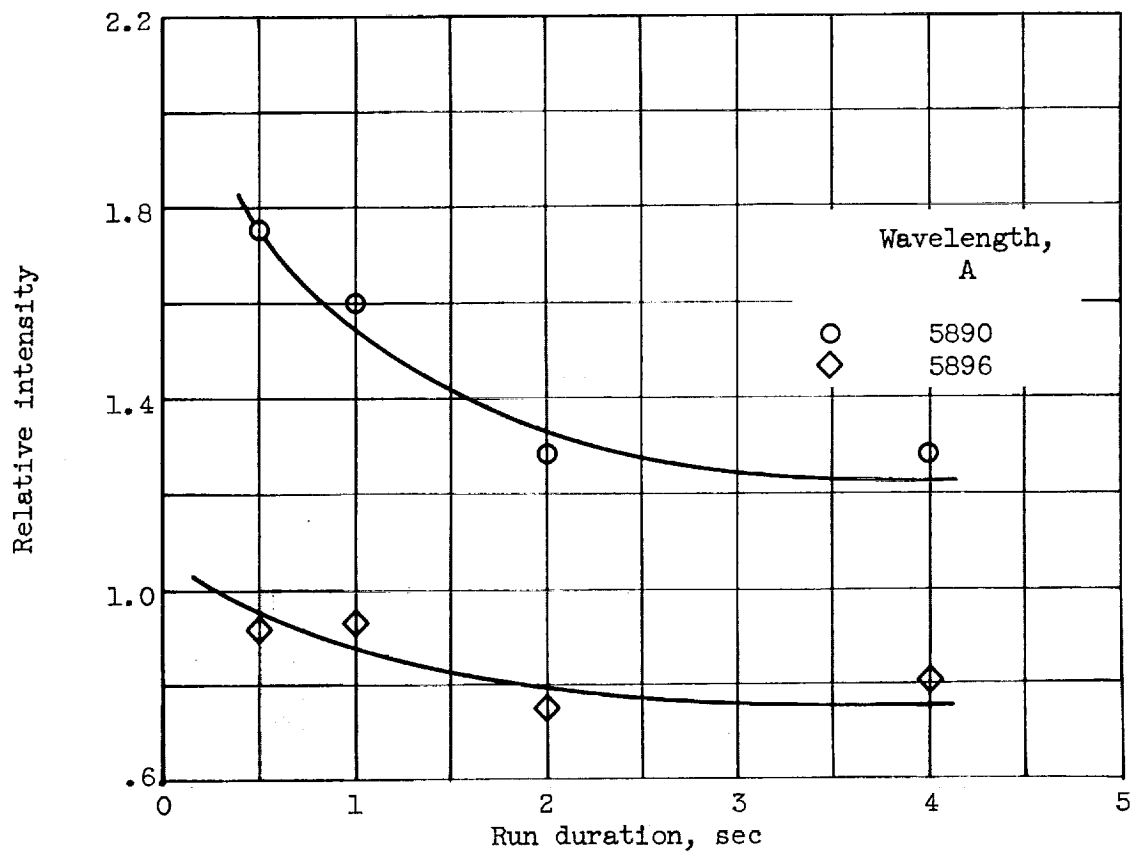


Figure 17. - Relative intensity of sodium emission as function of run length for five consecutive runs.

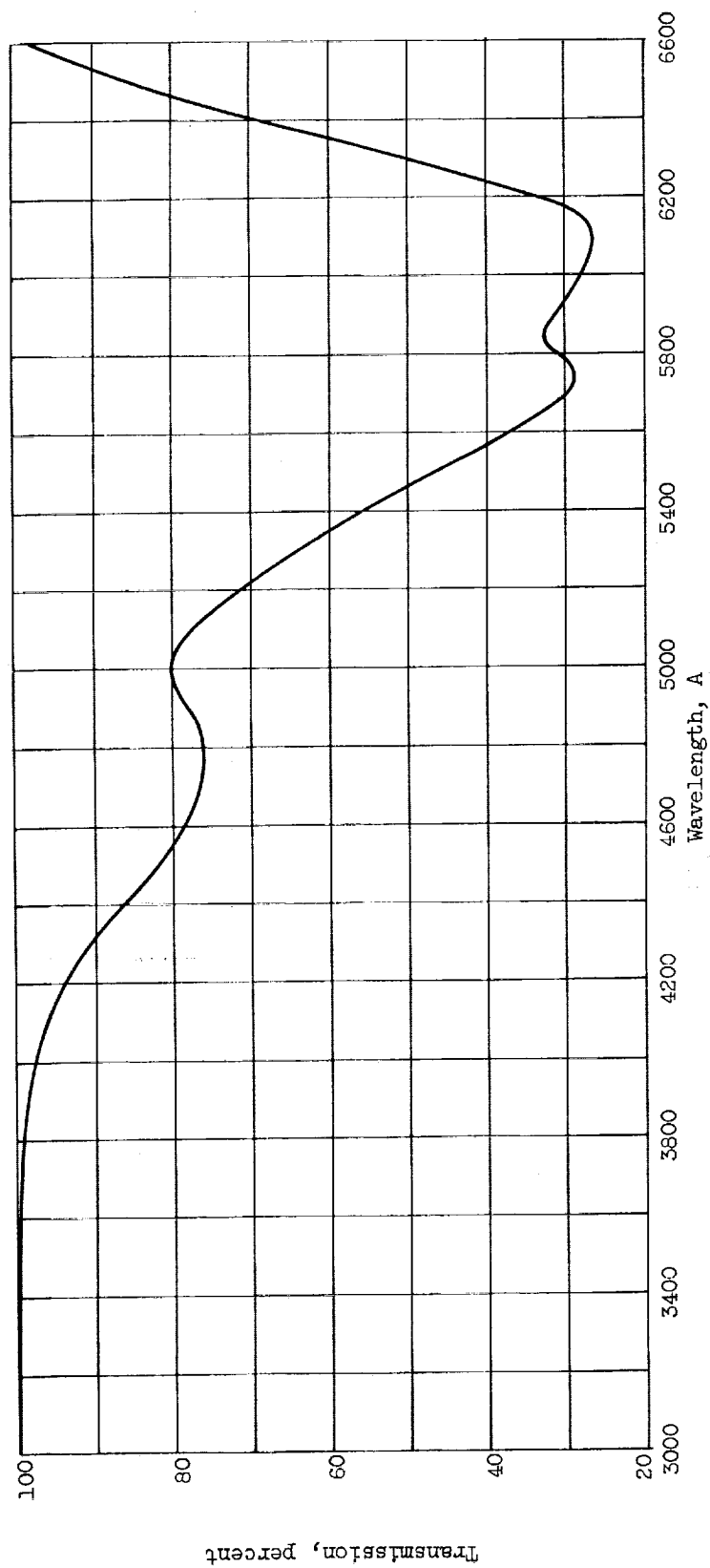


Figure 18. - Film calibration with tungsten filament at 2100° K.

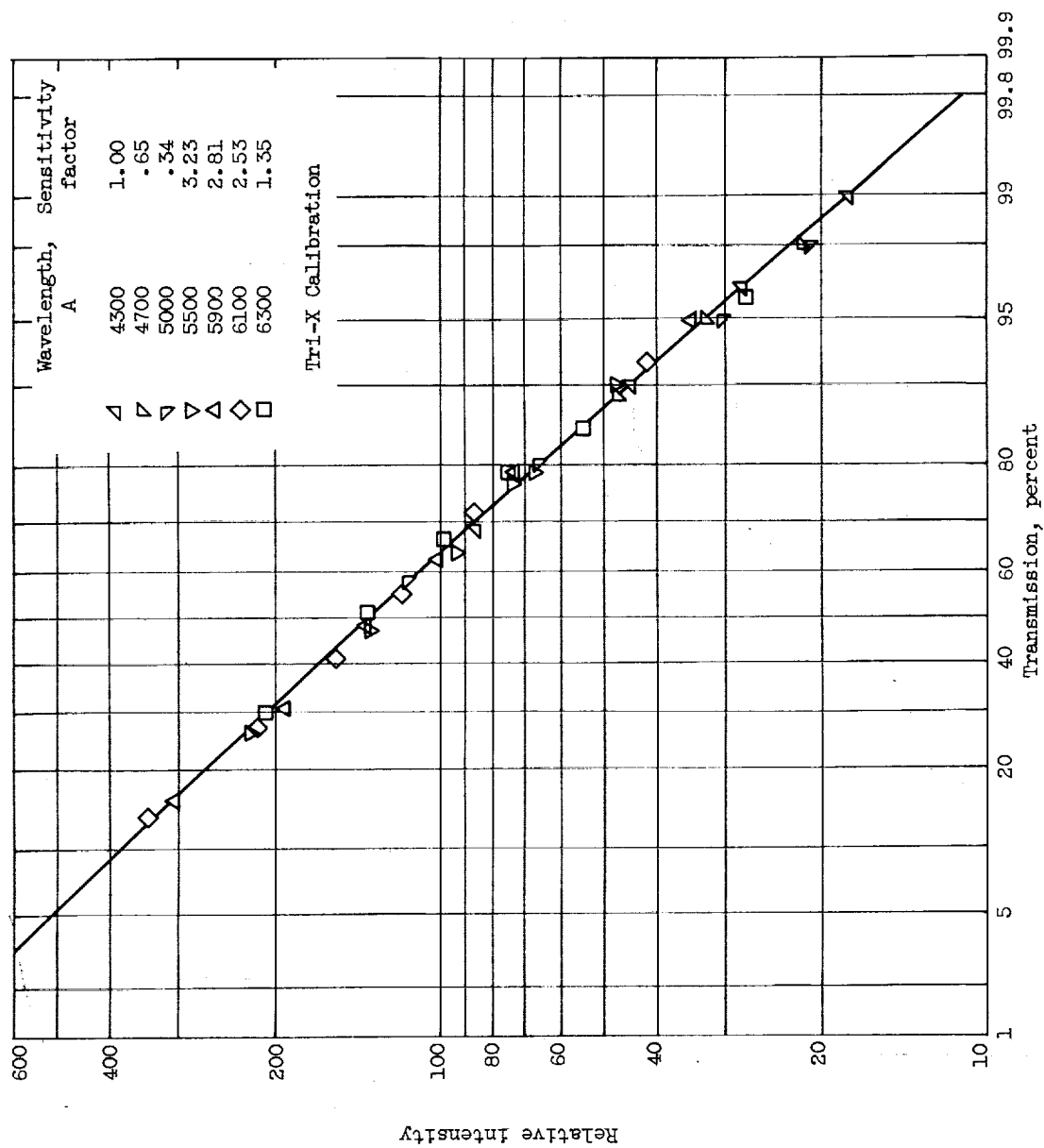


Figure 19. - Variation of radiation intensity at various wavelengths with transmission.

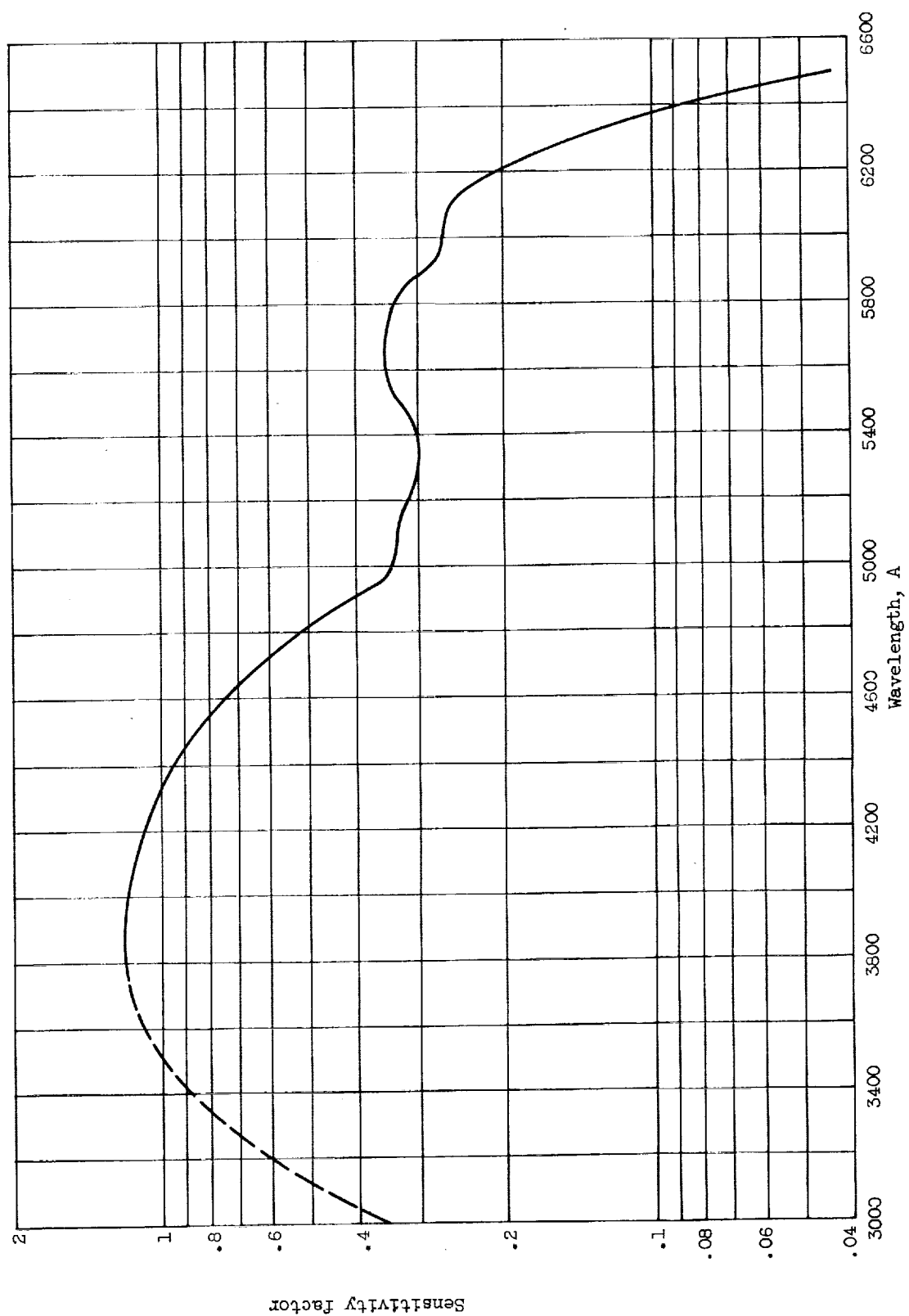


Figure 20. - Variation of sensitivity factor with wavelength.

<p>NASA TN D-1305 National Aeronautics and Space Administration. EMISSION SPECTRA FROM HIGH-PRESSURE HYDROGEN-OXYGEN COMBUSTION. Marshall C. Burrows and Louis A. Povinelli. July 1962. 36p. OTS price, \$1.00. (NASA TECHNICAL NOTE D-1305)</p> <p>Spectral radiation was evaluated from a nominal 200-lb-thrust hydrogen-rich hydrogen-oxygen combustor for the wavelength range 2100 to 7800 angstroms. Principal radiation consisted of the OH bands, the Schumann-Runge O₂ bands, the sodium D lines at 5890 and 5896 angstroms, and a continuum over the entire range. The intensities of OH, O₂, and the continuum radiation increased in proportion to both the oxidant-fuel weight ratio and the pressure. The results obtained are compared with those found in the literature and a statistical theory. The rotational temperature of the OH radical was evaluated, and the width of an OH line was determined. The behavior and the origin of sodium emission are also discussed.</p>	<p>I. Burrows, Marshall C. II. Povinelli, Louis A. III. NASA TN D-1305 (Initial NASA distribution: 30, Physics, atomic and molecular; 43, Propulsion systems, other; 44, Propulsion systems, theory.)</p> <p>NASA</p>	<p>NASA TN D-1305 National Aeronautics and Space Administration. EMISSION SPECTRA FROM HIGH-PRESSURE HYDROGEN-OXYGEN COMBUSTION. Marshall C. Burrows and Louis A. Povinelli. July 1962. 36p. OTS price, \$1.00. (NASA TECHNICAL NOTE D-1305)</p> <p>Spectral radiation was evaluated from a nominal 200-lb-thrust hydrogen-rich hydrogen-oxygen combustor for the wavelength range 2100 to 7800 angstroms. Principal radiation consisted of the OH bands, the Schumann-Runge O₂ bands, the sodium D lines at 5890 and 5896 angstroms, and a continuum over the entire range. The intensities of OH, O₂, and the continuum radiation increased in proportion to both the oxidant-fuel weight ratio and the pressure. The results obtained are compared with those found in the literature and a statistical theory. The rotational temperature of the OH radical was evaluated, and the width of an OH line was determined. The behavior and the origin of sodium emission are also discussed.</p>	<p>I. Burrows, Marshall C. II. Povinelli, Louis A. III. NASA TN D-1305 (Initial NASA distribution: 30, Physics, atomic and molecular; 43, Propulsion systems, other; 44, Propulsion systems, theory.)</p> <p>NASA</p>
<p>NASA TN D-1305 National Aeronautics and Space Administration. EMISSION SPECTRA FROM HIGH-PRESSURE HYDROGEN-OXYGEN COMBUSTION. Marshall C. Burrows and Louis A. Povinelli. July 1962. 36p. OTS price, \$1.00. (NASA TECHNICAL NOTE D-1305)</p> <p>Spectral radiation was evaluated from a nominal 200-lb-thrust hydrogen-rich hydrogen-oxygen combustor for the wavelength range 2100 to 7800 angstroms. Principal radiation consisted of the OH bands, the Schumann-Runge O₂ bands, the sodium D lines at 5890 and 5896 angstroms, and a continuum over the entire range. The intensities of OH, O₂, and the continuum radiation increased in proportion to both the oxidant-fuel weight ratio and the pressure. The results obtained are compared with those found in the literature and a statistical theory. The rotational temperature of the OH radical was evaluated, and the width of an OH line was determined. The behavior and the origin of sodium emission are also discussed.</p>	<p>I. Burrows, Marshall C. II. Povinelli, Louis A. III. NASA TN D-1305 (Initial NASA distribution: 30, Physics, atomic and molecular; 43, Propulsion systems, other; 44, Propulsion systems, theory.)</p> <p>NASA</p>	<p>NASA TN D-1305 National Aeronautics and Space Administration. EMISSION SPECTRA FROM HIGH-PRESSURE HYDROGEN-OXYGEN COMBUSTION. Marshall C. Burrows and Louis A. Povinelli. July 1962. 36p. OTS price, \$1.00. (NASA TECHNICAL NOTE D-1305)</p> <p>Spectral radiation was evaluated from a nominal 200-lb-thrust hydrogen-rich hydrogen-oxygen combustor for the wavelength range 2100 to 7800 angstroms. Principal radiation consisted of the OH bands, the Schumann-Runge O₂ bands, the sodium D lines at 5890 and 5896 angstroms, and a continuum over the entire range. The intensities of OH, O₂, and the continuum radiation increased in proportion to both the oxidant-fuel weight ratio and the pressure. The results obtained are compared with those found in the literature and a statistical theory. The rotational temperature of the OH radical was evaluated, and the width of an OH line was determined. The behavior and the origin of sodium emission are also discussed.</p>	<p>I. Burrows, Marshall C. II. Povinelli, Louis A. III. NASA TN D-1305 (Initial NASA distribution: 30, Physics, atomic and molecular; 43, Propulsion systems, other; 44, Propulsion systems, theory.)</p> <p>NASA</p>

